

**Evaluation of a Low-Temperature Single-Axis Force  
Sensor for the MSL SA/SPaH Subsystem**

**JPL Technical Report: D-35482**

**Daniel Helmick and Matt DiCicco**

**2/2/2006**

# 1 Introduction

The purpose of the experiment and analysis described in this document is to evaluate the performance and function of a custom-designed, single-axis force sensor in a low-temperature environment. The sensor is tested across the assumed temperature and force operational ranges of the Mars Science Laboratory (MSL) Sample Acquisition/Sample Processing and Handling (SA/SPaH) subsystem. Ground truth force is used to quantitatively evaluate accuracy, repeatability, temperature dependence, hysteresis, and functionality.

In *Section 2*, the experimental setup is described. It gives the details of the hardware and software configuration that is used to collect the experimental data. In *Section 3*, the experimental procedure is described. It gives the steps followed to achieve the experimental results. In *Section 4*, the experimental results are shown. The data are plotted and organized in a manner such that conclusions relevant to the application can be drawn. In *Section 5*, conclusions that impact the SA/SPaH subsystem are described. In *Appendix A*, post-experiment x-ray results are shown in an attempt to compare an untested sensor with a tested sensor in order to detect any degradation in the tested sensor. Data sheets for the force sensors are included in *Appendix B* and *Appendix C*. Calibration certificates for the two sensors can be found in *Appendix D* and *Appendix E*.

## 2 Experimental Setup

The test apparatus consists of two force sensors and a thermocouple mounted to a rigid frame (see Figure 1 and Figure 2). The frame is designed to fit through the opening in a cryogenic thermal test chamber such that one sensor is maintained at room temperature and the other is maintained at the chamber temperature. The two force sensors are connected with a rigid connecting rod and the warm sensor is also connected to a force application mechanism. This device uses springs to apply a smooth, predictable force that can be varied by hand-turning a knob connected to a lead screw. The apparatus is mounted horizontally to minimize gravity effects. Any parts which pass through the thermal chamber wall are made from carbon fiber composite in order to thermally isolate the two halves of the device.

The *room temperature* force sensor is a Futek LRF325 (part no. FSH00075) (see *Appendix B*). This single-axis force sensor remains at room temperature throughout the entire experimental procedure. Its output is treated as ground truth and it has a range of  $\pm 333\text{N}$  (75 lbf). The *cryogenic* force sensor is a custom-designed Futek QLA246 (part # QSH00626) (serial # 205689) (see *Appendix C*). It uses modified encapsulated Karma strain gages with special polyimide backing to remain functional at low temperatures. This sensor resides in the cryogenic chamber throughout the experiments with its temperature varying between each test as described in *Section 3*. It has a range of  $\pm 250\text{N}$  (56 lbf) and is specified to be temperature compensated down to  $-80^{\circ}\text{C}$ . Both sensors are rated to measure both tensile and compressive forces. To measure the temperature of the cryogenic force sensor a thermocouple is installed next to the sensor. This thermocouple is a type T thermocouple with a range of  $-200^{\circ}\text{C}$  to  $400^{\circ}\text{C}$ .

All three sensors are calibrated. The two force sensors are calibrated at Futek using NIST calibration procedures and are certified. The results of these calibrations are 3<sup>rd</sup> order polynomial fits that reduce the measurement error to <0.2% of full scale at room temperature. The thermocouple is calibrated with a handheld thermocouple calibrator (Omega CL20 series). The result is a measurement that is accurate to within 0.3°C.

A signal conditioning and data acquisition system is used to collect the data during the experiments. This system consists of National Instruments signal conditioning units specifically designed for force sensors and thermocouples. The SCC-SG04 is designed for full-bridge strain gage force sensors. It amplifies (x100) and filters (1.6 kHz single pole RC low pass) the signals from each of the force sensors. The SCC-TC is designed for thermocouples. It amplifies (x100), filters (2 Hz dual pole low pass), and compensates for cold junction effects using a local thermistor. A National Instruments 6036E A/D card is used for the analog to digital conversion of the signals. This card uses 16 bit conversion with software settable pre-amps. A laptop running Fedora Core 4 (Linux kernel 2.6.12), Comedi hardware drivers ([www.comedi.org](http://www.comedi.org)), and a custom data acquisition/conversion/logging/display program is used to collect, store, and display all data continuously at 10 Hz throughout all experiments.

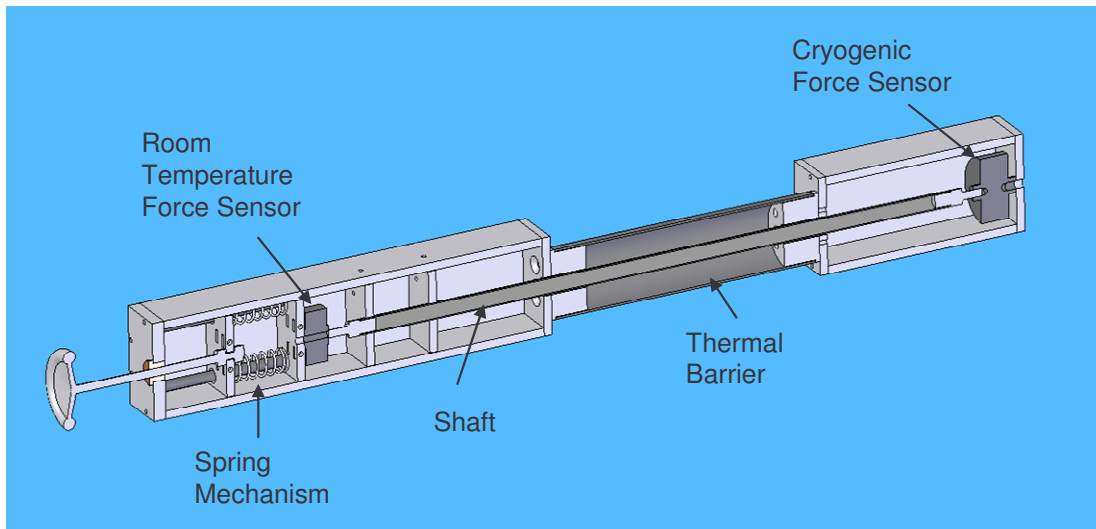


**Figure 1:** Cutaway drawing of test apparatus

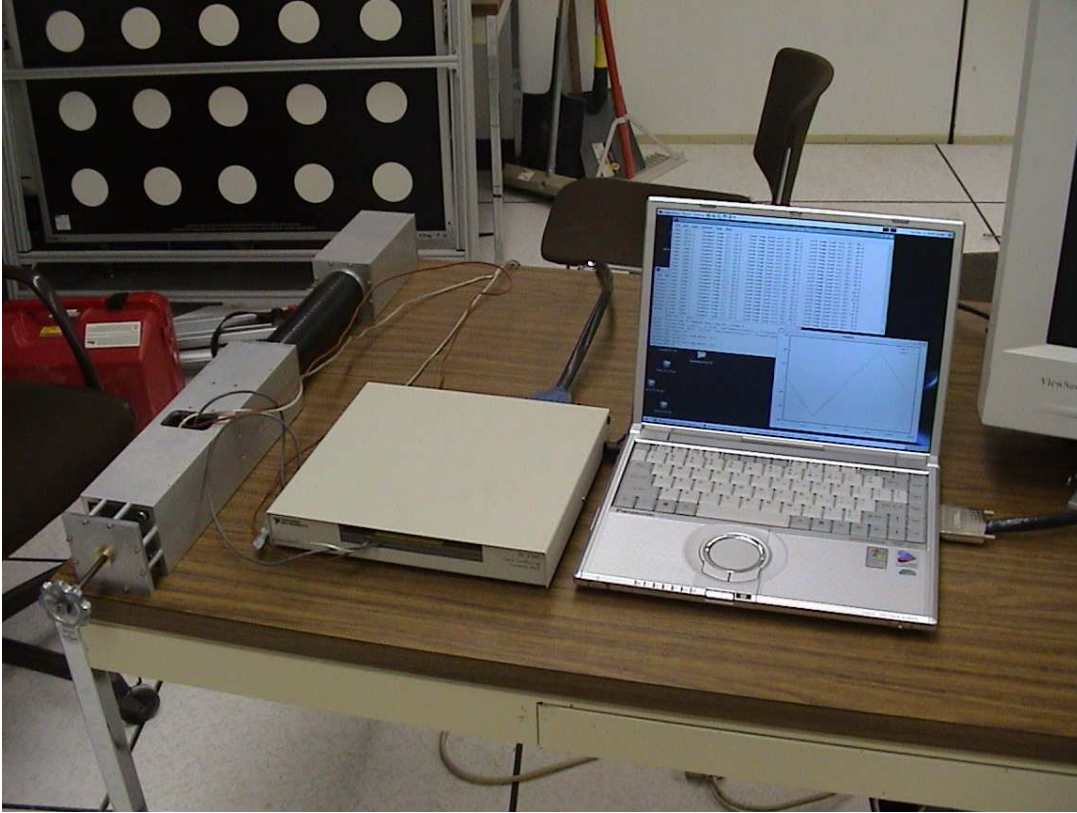


**Figure 2:** Final assembly with data acquisition hardware

### 3 Experimental Procedure

The procedure is to apply identical loads to the *room temperature* force sensor and the *cryogenic* force sensor through a testing apparatus. The end of this apparatus containing the cryogenic force sensor is placed within a cryogenic chamber where its temperature can be varied within the range of  $+100^{\circ}\text{C}$  to  $-135^{\circ}\text{C}$ .

Functional tests are performed at various temperatures using the apparatus. These tests consist of ramping the applied force from  $0\text{N}$  down to  $-250\text{N}$ , up to  $+250\text{N}$  and back down to  $0\text{N}$ . At each  $10\text{N}$  increment the force is held constant for 10 seconds in order to remove any dynamical effects on the data (any of which are presumed to be extremely fast and easily taken care of by this length pause). This test is first performed at room temperature and then the temperature is lowered in  $\sim 20^{\circ}\text{C}$  increments and the test is repeated down to  $-70^{\circ}\text{C}$ . To assess hysteretic effects and to avoid rapid warming, the chamber is warmed back to room temperature, again in  $\sim 20^{\circ}\text{C}$  increments, with functional tests performed at each increment.

To assess the survivability of the force sensor, a deep cycle test is performed after each battery of functional tests. The deep cycle consists of raising the temperature of the sensor to  $+100^{\circ}\text{C}$  for one hour followed by lowering the temperature to  $-135^{\circ}\text{C}$  for one hour. The sensor is not loaded during these tests, but room temperature functional tests are performed after each deep cycle to confirm functionality.

In all, there are three batteries of functional tests with a deep cycle performed at the conclusion of each. After the final deep cycle, one additional room temperature functional test is performed to ensure that the force sensor is still functional.

A detailed description of the steps in this procedure is as follows:

1. Assemble test rig and begin data collection software. This software samples the chamber temperature, forces of the two force sensors, and timestamps at 10Hz. Turn on the thermal chamber and set it to room temperature ( $\sim 23^{\circ}\text{C}$ ). Turn on the nitrogen purge to remove all moisture from the chamber.
2. Zero out the forces on the force sensors (with the lead screw knob) and verify all signals are being recorded properly.
3. Perform one functional test:
  - a. Ramp load on apparatus down to  $-250\text{N}$  (compression) at 10N increments. After achieving the new force level, wait for 10 seconds
  - b. Ramp load on apparatus back to  $0\text{N}$ , again at 10N increments with 10 second pauses at each level
  - c. Ramp load on apparatus up to  $+250\text{N}$  (tension) in the same manner
  - d. Ramp load on apparatus down to  $0\text{N}$  in the same manner
4. Repeat steps 2 and 3 with the thermal chamber set to the following values (in this order):  $5^{\circ}\text{C}$ ,  $-15^{\circ}\text{C}$ ,  $-35^{\circ}\text{C}$ ,  $-55^{\circ}\text{C}$ ,  $-70^{\circ}\text{C}$ ,  $-55^{\circ}\text{C}$ ,  $-35^{\circ}\text{C}$ ,  $-15^{\circ}\text{C}$ ,  $5^{\circ}\text{C}$ , and room temperature. At each temperature, wait for the chamber to reach steady state temperature before performing any tests.
5. Perform a deep cycle test as follows:
  - a. Remove the apparatus from the chamber and remove the force sensor. Place the force sensor in the chamber by itself and seal the chamber.
  - b. Set chamber temperature to  $110^{\circ}\text{C}$
  - c. Allow to sit for 1 hour after chamber reaches temperature
  - d. Reset chamber temperature to  $-135^{\circ}\text{C}$
  - e. Allow to sit for 1 hour after chamber reaches temperature
  - f. Return chamber to room temperature
6. Repeat steps 1-5 three times.
7. After the completion of the third deep cycle, perform step 3 as a final functional test.

## 4 Results

This section shows the results for the three test runs performed. At the start of each subsection, information about the test is provided. This information includes the day the test was performed, notes about deep cycles performed, and any anomalies noted during the test.

*Figure 3 - Figure 13, Figure 5 - Figure 25, and Figure 27 - Figure 37:*

For each functional test, a force plot which shows the force signals from the room temperature and cryogenic sensors is shown. In each plot, the red line represents the

room temperature sensor which is considered to be the ground truth force value. The blue line represents the force from the temperature compensated sensor inside the chamber. The staircase-like shape of the curves is from the 10 second pause performed at each 10N increment.

*Figure 14, Figure 26, and Figure 38:*

The force error (the difference between the outputs from the two force sensors) from each of the functional tests was analyzed and included on one graph to observe any relationship between error and temperature. Each of these figures plots the mean force error vs. the mean temperature for that day's range of functional tests. This data is separated into two categories: cooling and warming. Cooling tests are the tests performed as the temperature was lowered from room temperature down to  $-70^{\circ}\text{C}$ . Warming tests are those performed as the temperature was raised from  $-70^{\circ}\text{C}$  back to room temperature.

In section 4.4, the results of all three batteries of tests are combined and additional results plots and tables are included and discussed.

## 4.1 Test 1

Test date: 12/7/2005

New sensor, no tests performed prior to this test

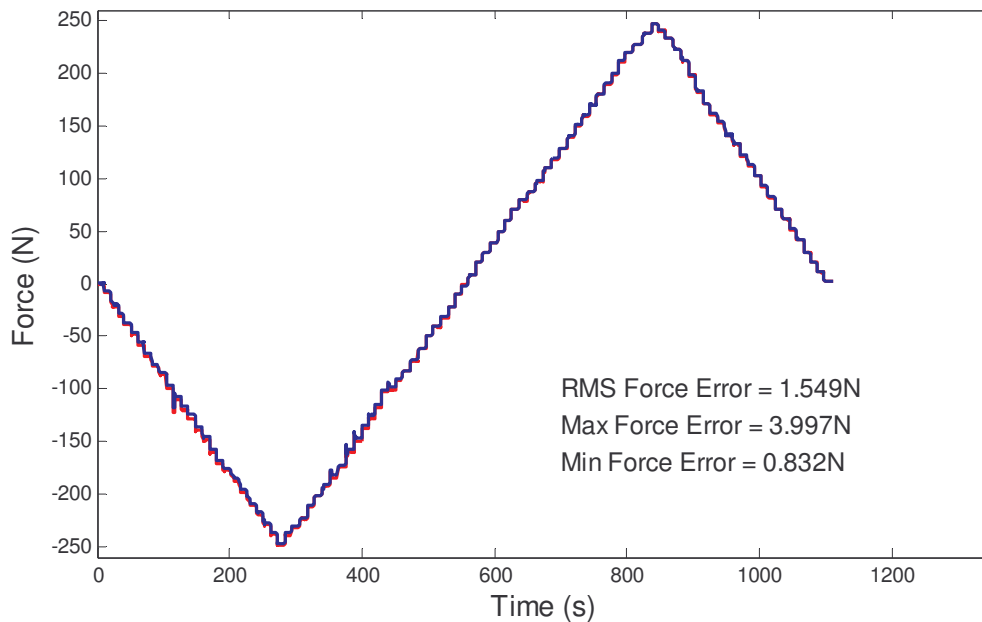


**Figure 3:** Test 1, room temperature (mean  $22.3^{\circ}\text{C}$ , std dev 0.15), cooling

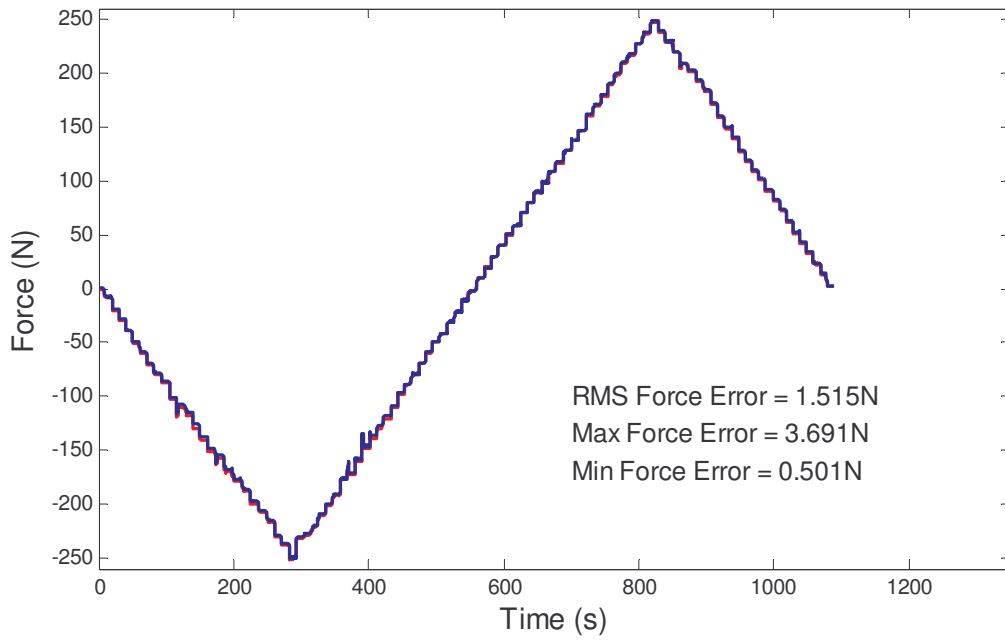


**Figure 4:** Test 1, 5°C (mean 6.6°C, std dev 0.10), cooling

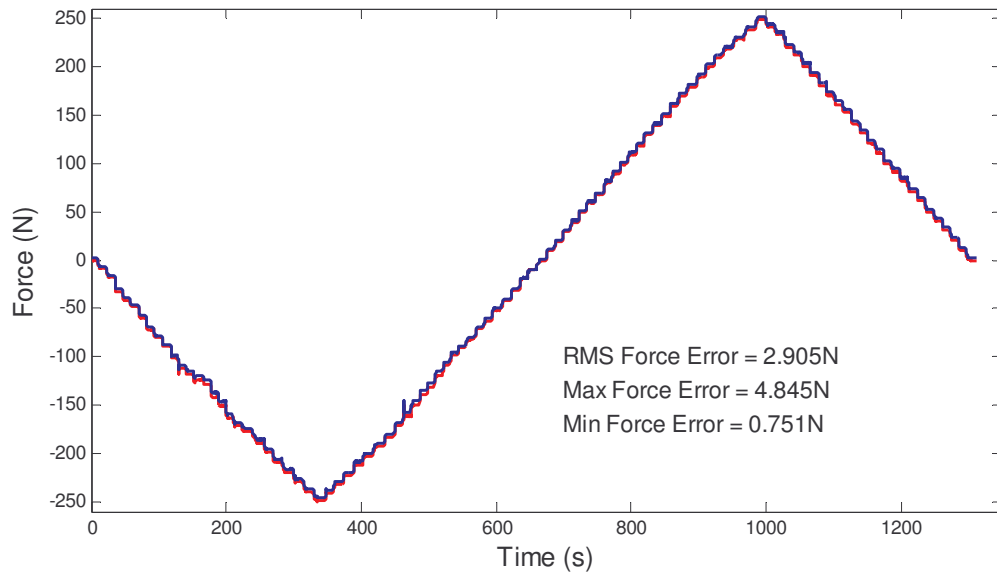


**Figure 5:** Test 1, -15°C (mean -13.9°C, std dev 0.21), cooling

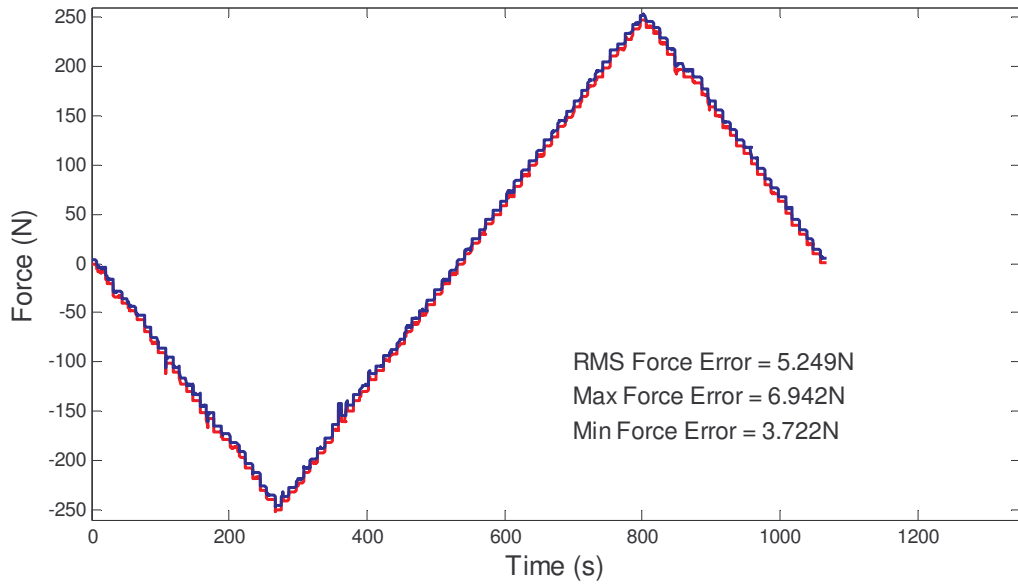


**Figure 6:** Test 1, -35°C (mean -41.6°C, std dev 0.53), cooling

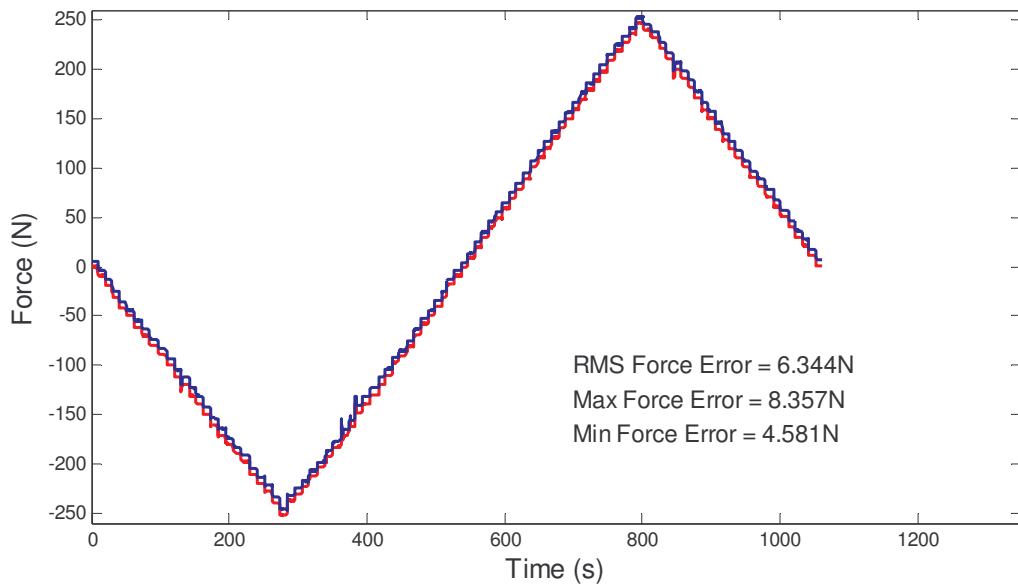


**Figure 7:** Test 1, -55°C (mean -60.0°C, std dev 0.77), cooling



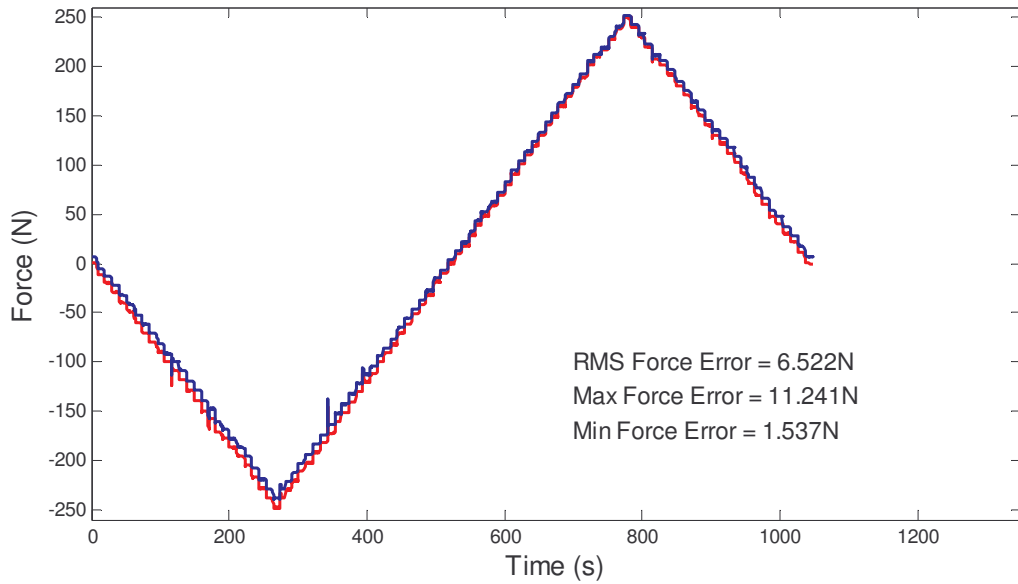


**Figure 8:** Test 1, -70°C (mean -69.6°C, std dev 0.53)

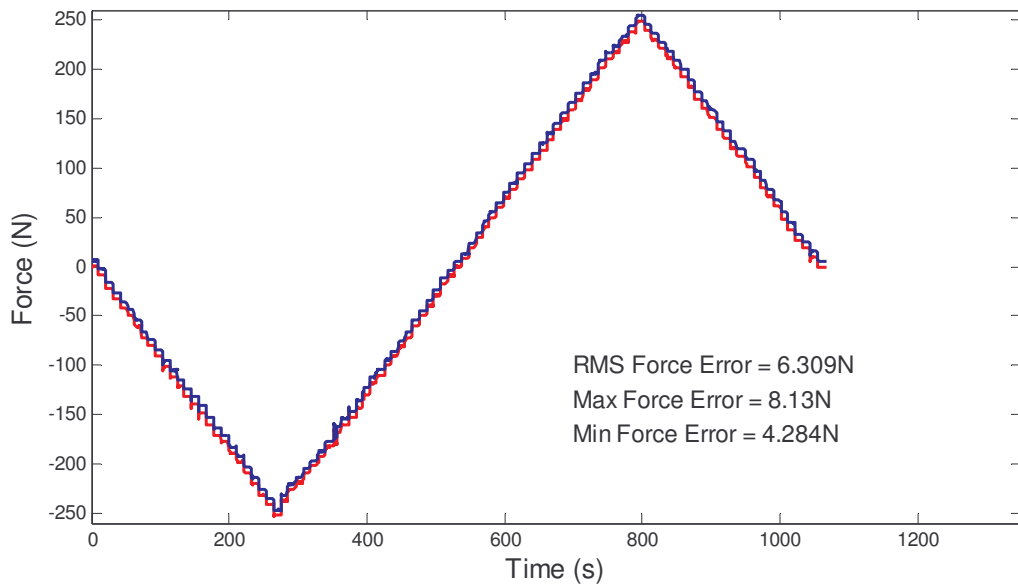


**Figure 9:** Test 1, -55°C (mean -55.0°C, std dev 0.09), warming

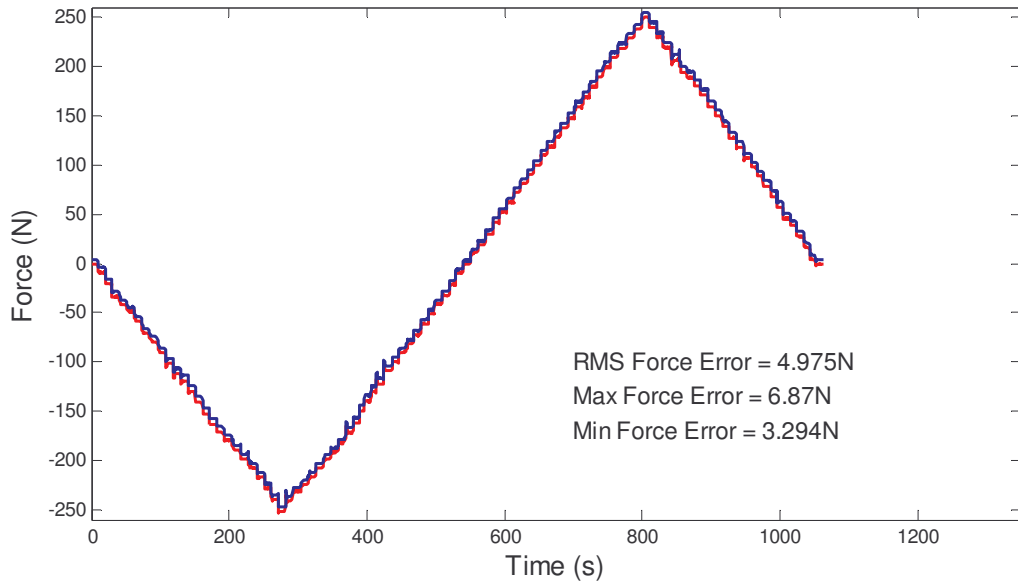


**Figure 10:** Test 1, -35°C (mean -35.2°C, std dev 0.96), warming

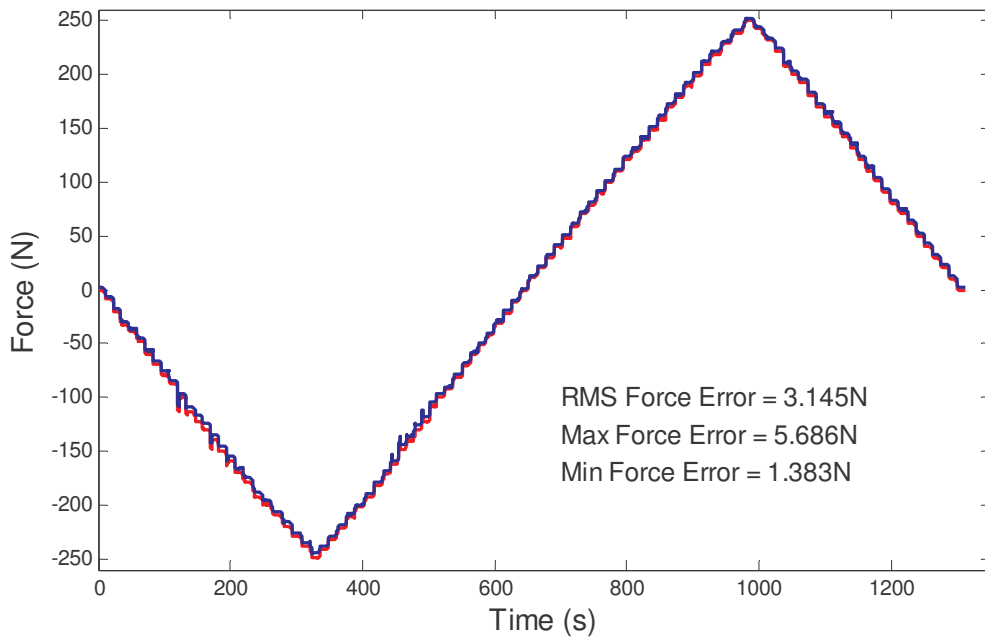


**Figure 11:** Test 1, -15°C (mean -10.6°C, std dev 0.28), warming

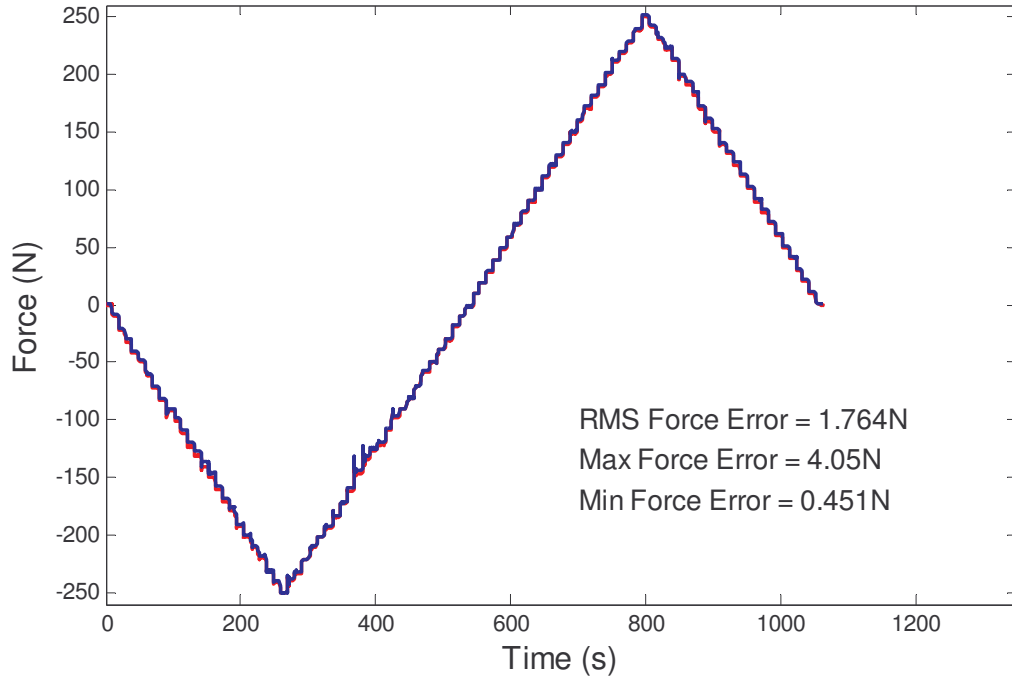


**Figure 12:** Test 1, 5°C (mean 6.2°C, std dev 0.14), warming

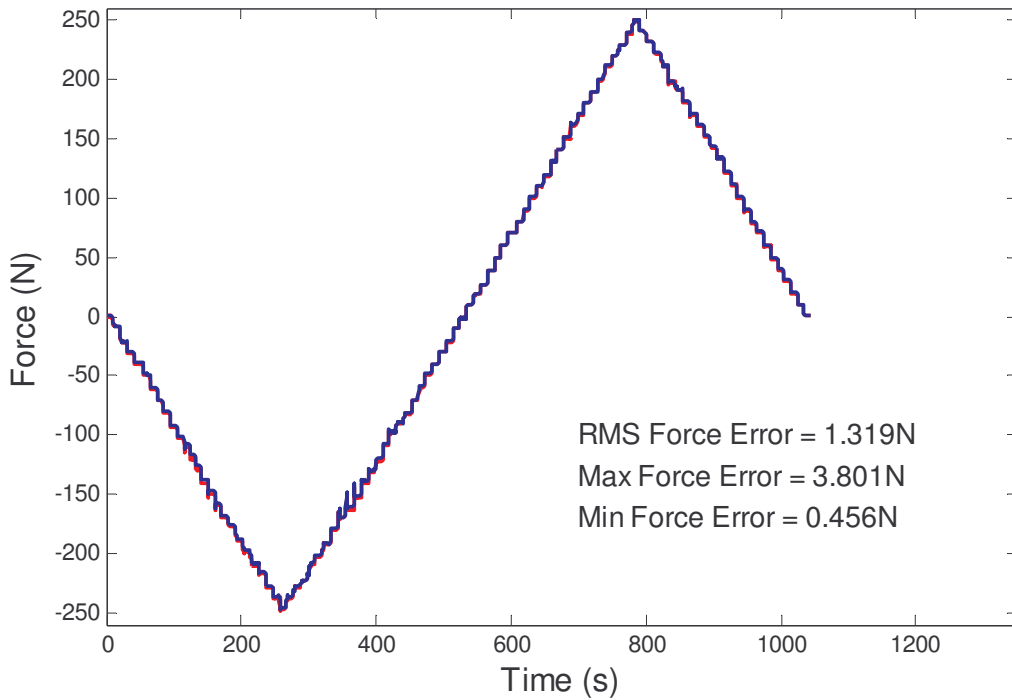


**Figure 13:** Test 1, room temperature (mean 21.4°C, std dev 0.26), warming

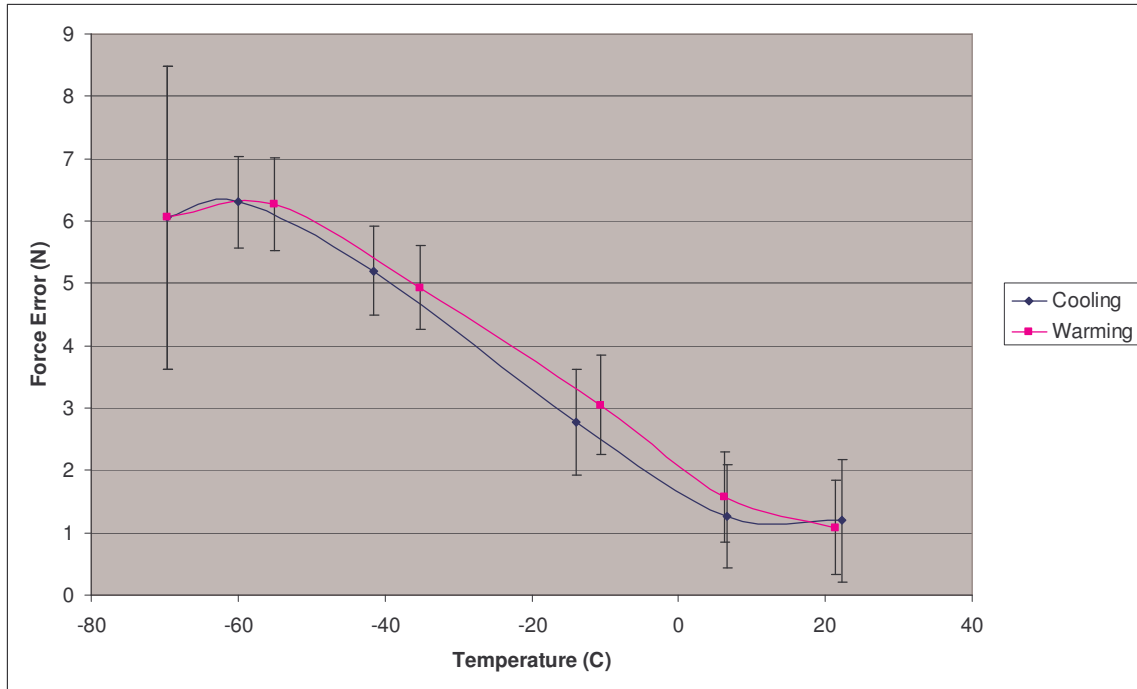


**Figure 14:** Test 1 summary of results

## 4.2 Test 2

Test date: 12/8/2005

Deep cycle #1 performed before this test on 12/8/2005

1 hour at +110°C, 1 hour at -135°C

### *Anomalies:*

During the second -15°C test, the chamber liquid NO<sub>2</sub> valve became frozen in the on position, dropping the chamber temperature momentarily below -20°C before being fixed. It can be noted that the standard deviation on this temperature is about 3°C, significantly larger than any other test in the experiment.

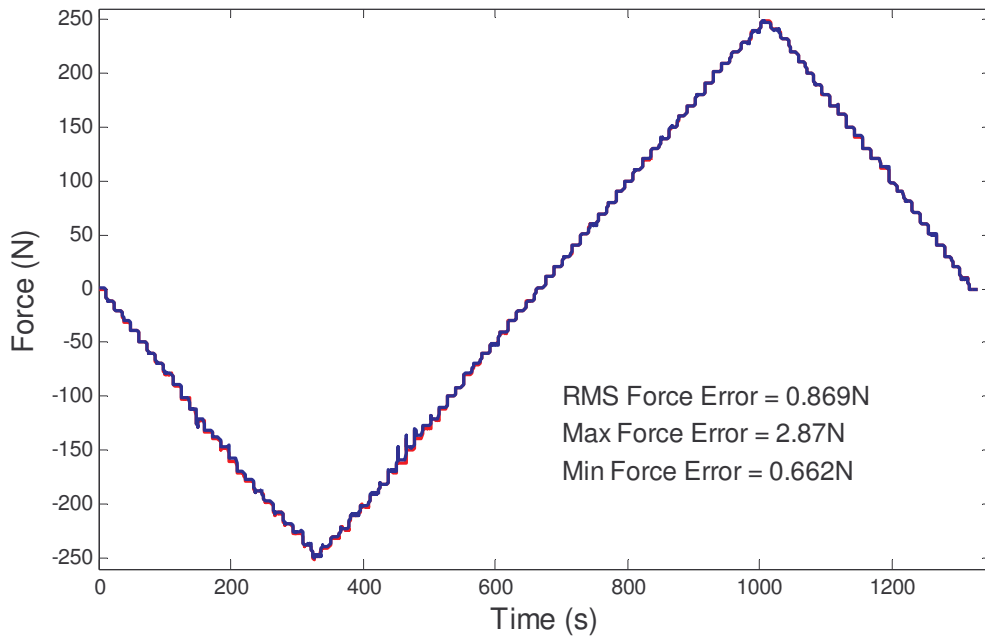


**Figure 15:** Test 2, room temperature (mean 24.8°C, std dev 0.67), cooling

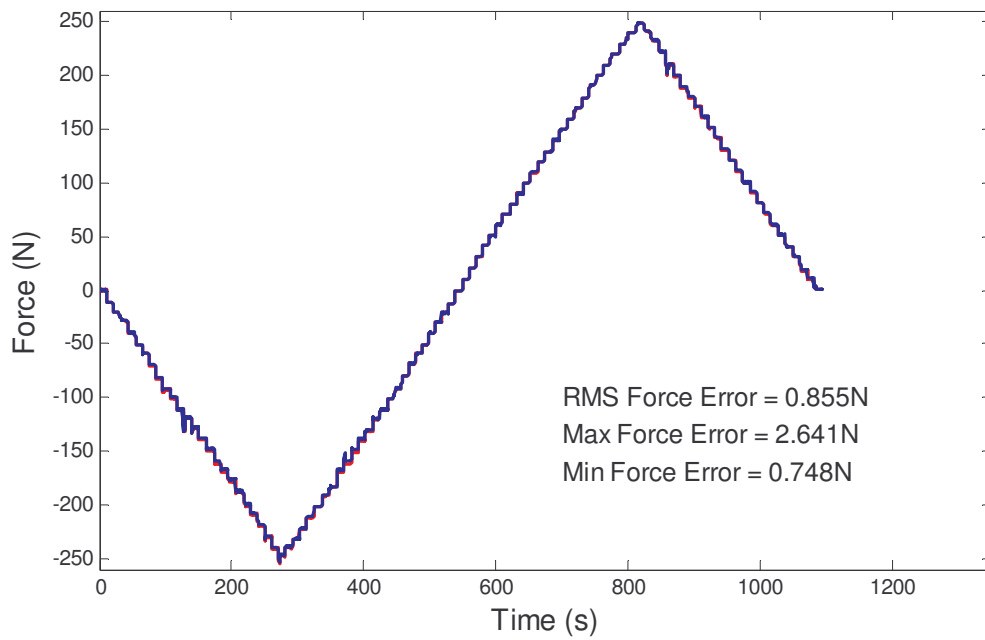


**Figure 16:** Test 2, 5°C (mean 6.7°C, std dev 0.19), cooling

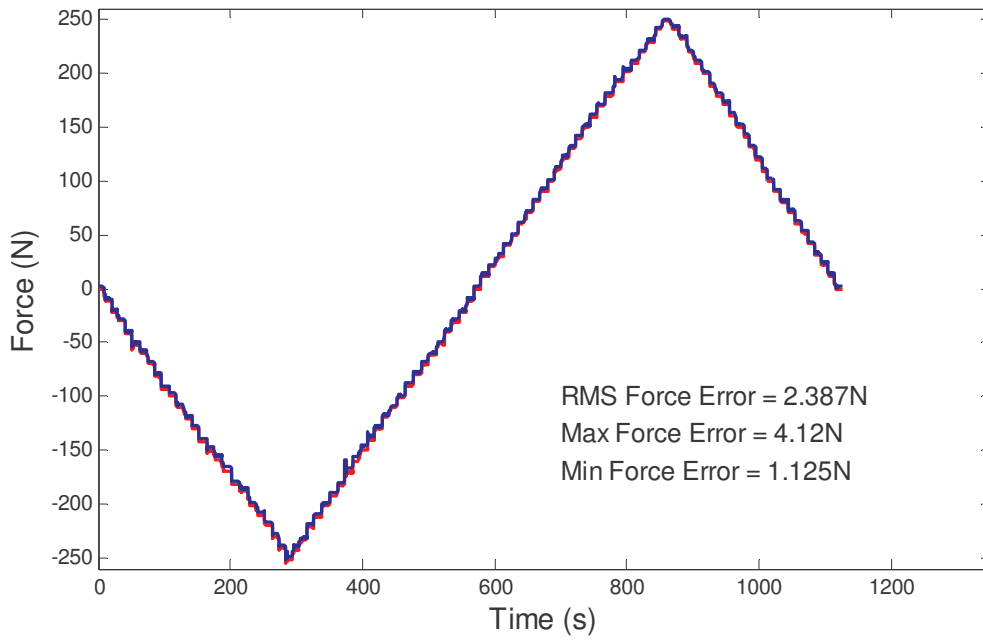


**Figure 17:** Test 2, -15°C (mean -16.1°C, std dev 0.52), cooling

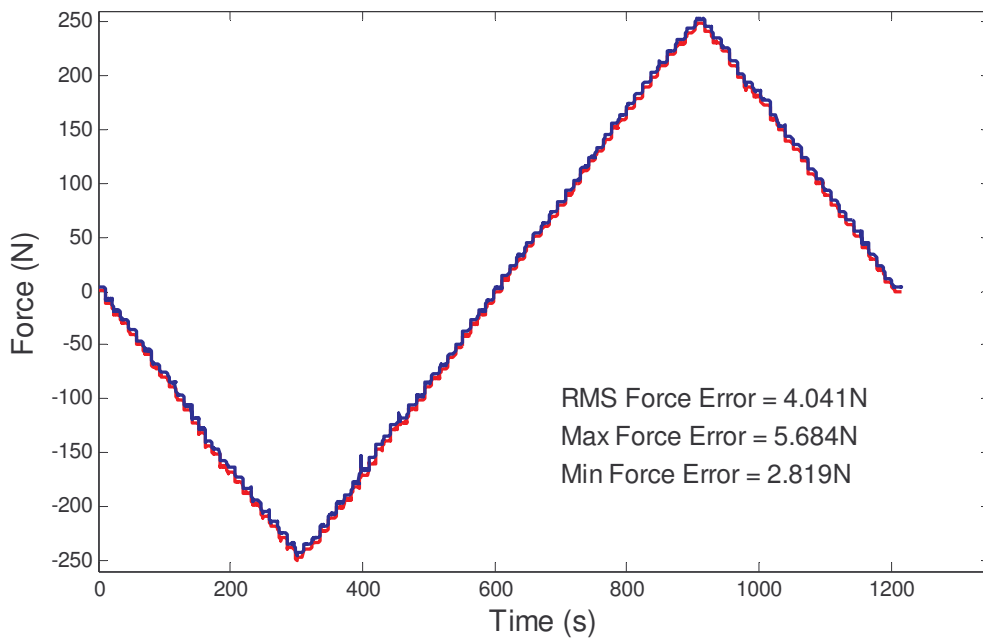


**Figure 18:** Test 2, -35°C (mean -37.3°C, std dev 0.38), cooling

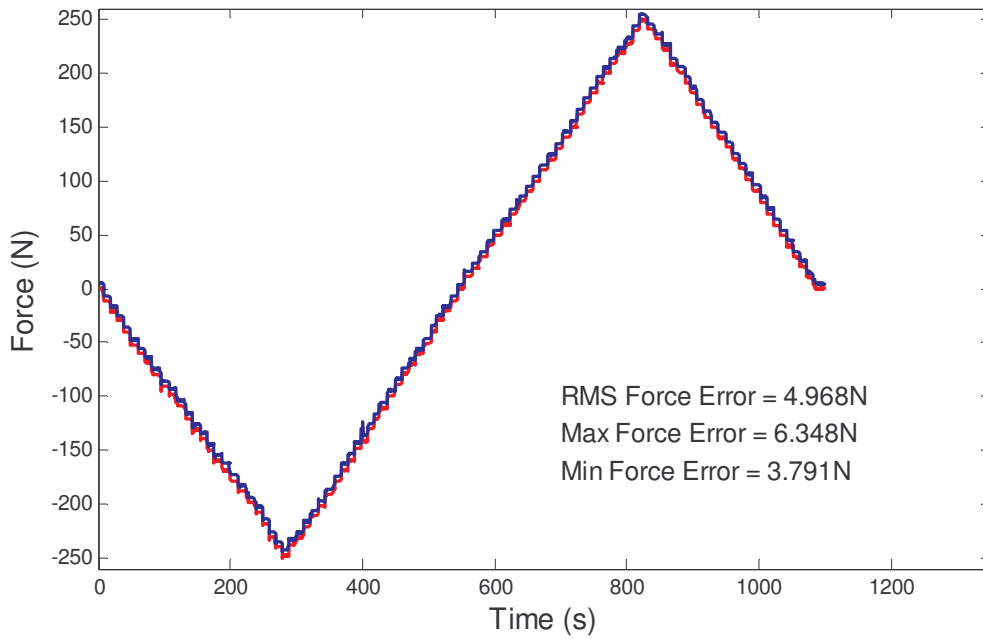


**Figure 19:** Test 2, -55°C (mean -55.1°C, std dev 0.08), cooling

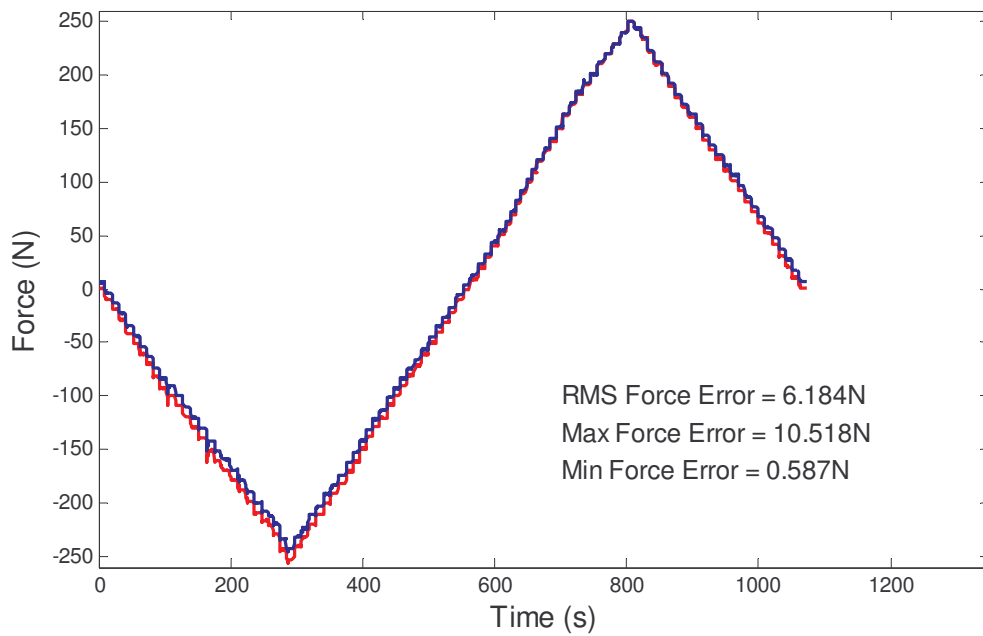


**Figure 20:** Test 2, -70°C (mean -73.1°C, std dev 0.13)

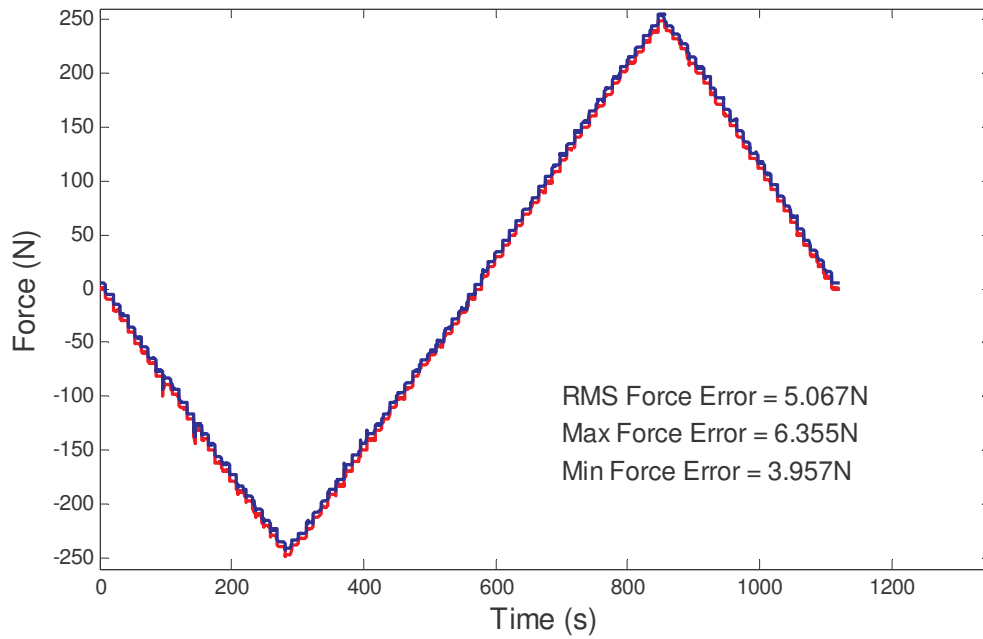


**Figure 21:** Test 2, -55°C (mean -53.8°C, std dev 0.2), warming

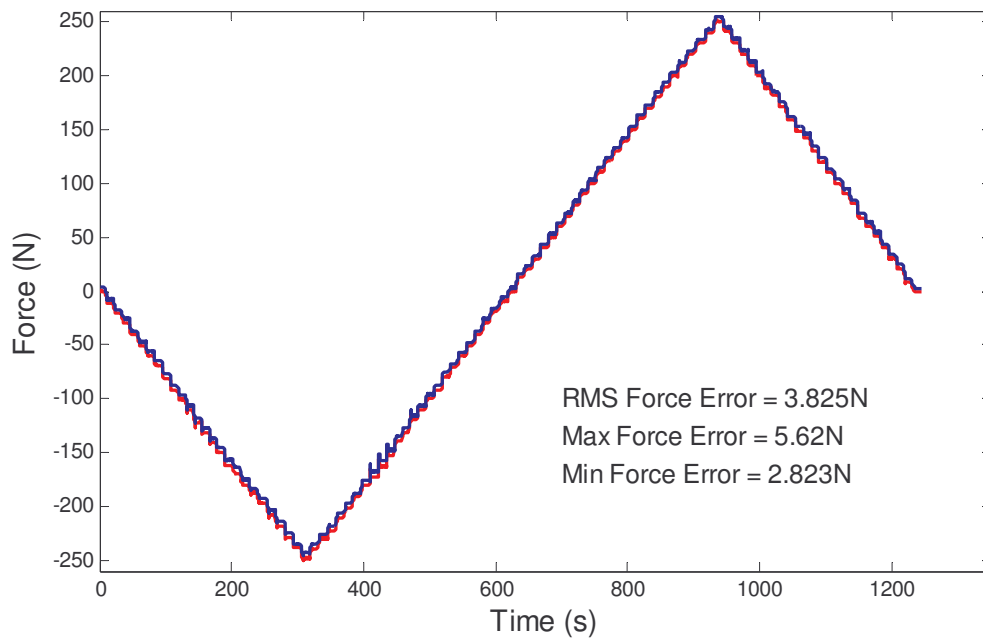


**Figure 22:** Test 2, -35°C (mean -33.1°C, std dev 0.16), warming



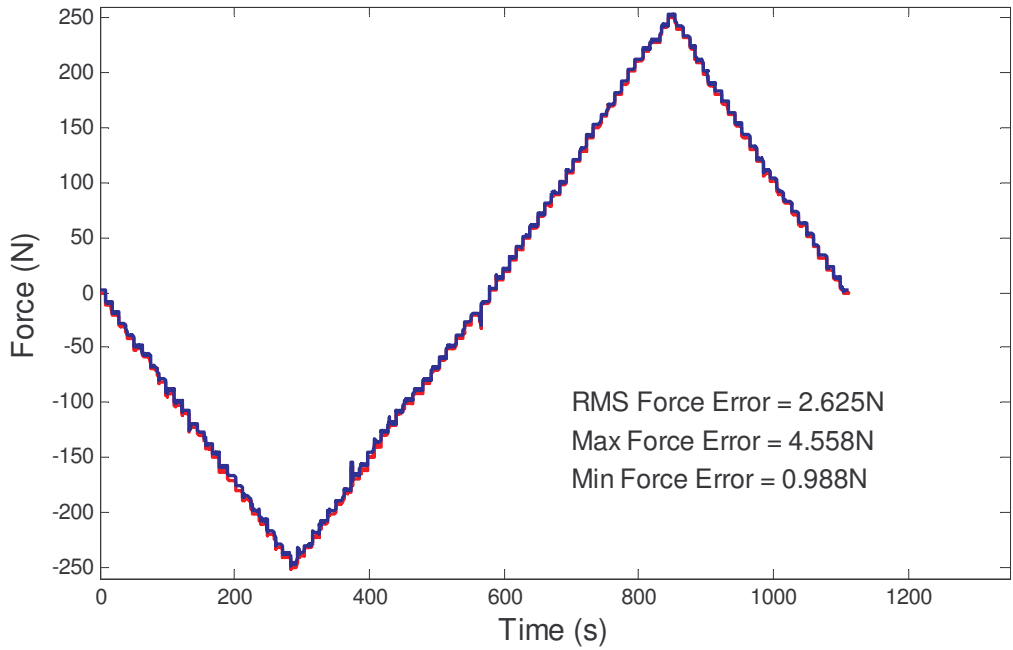


**Figure 23:** Test 2, -15°C (mean -17.5°C, std dev 3.04), warming

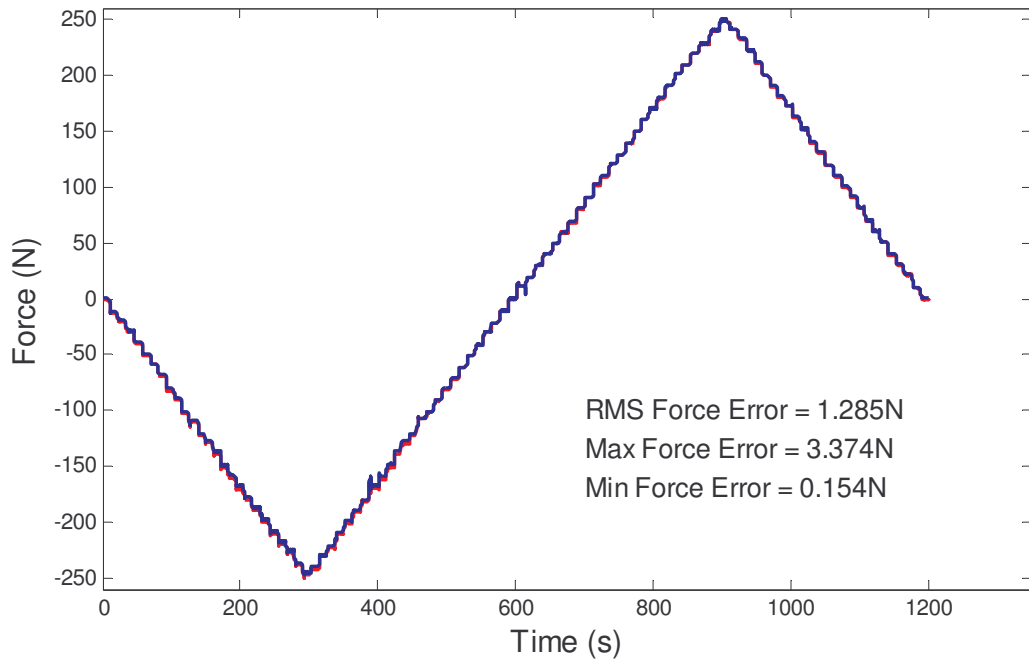


**Figure 24:** Test 2, 5°C (mean 6.1°C, std dev 0.38), warming

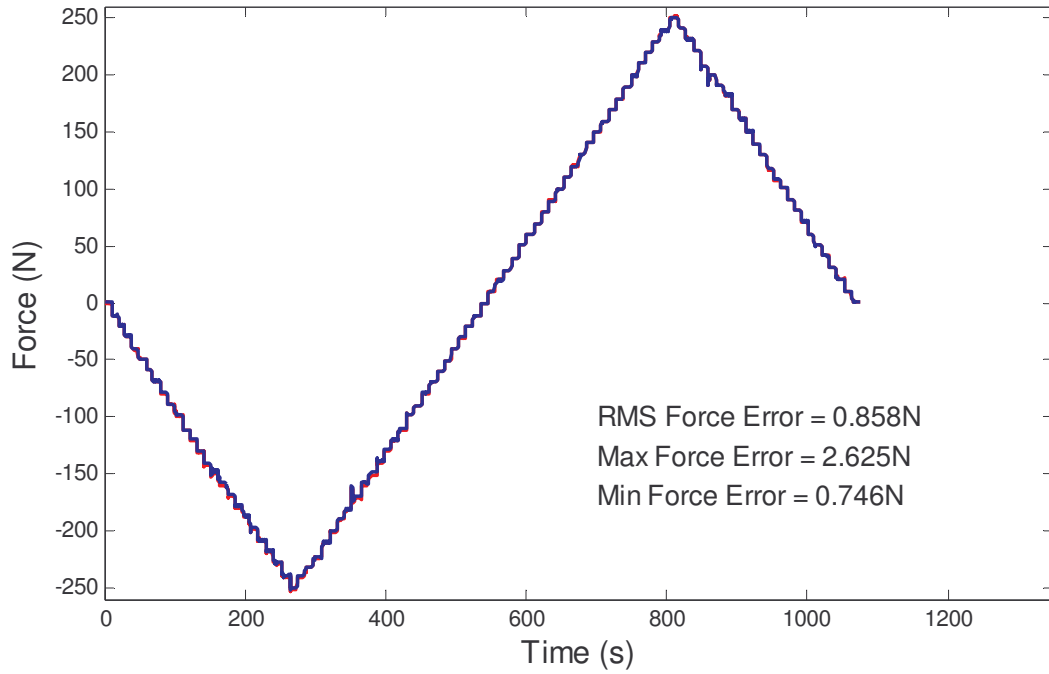


**Figure 25:** Test 2, room temperature (mean 25.4°C, std dev 0.76), warming

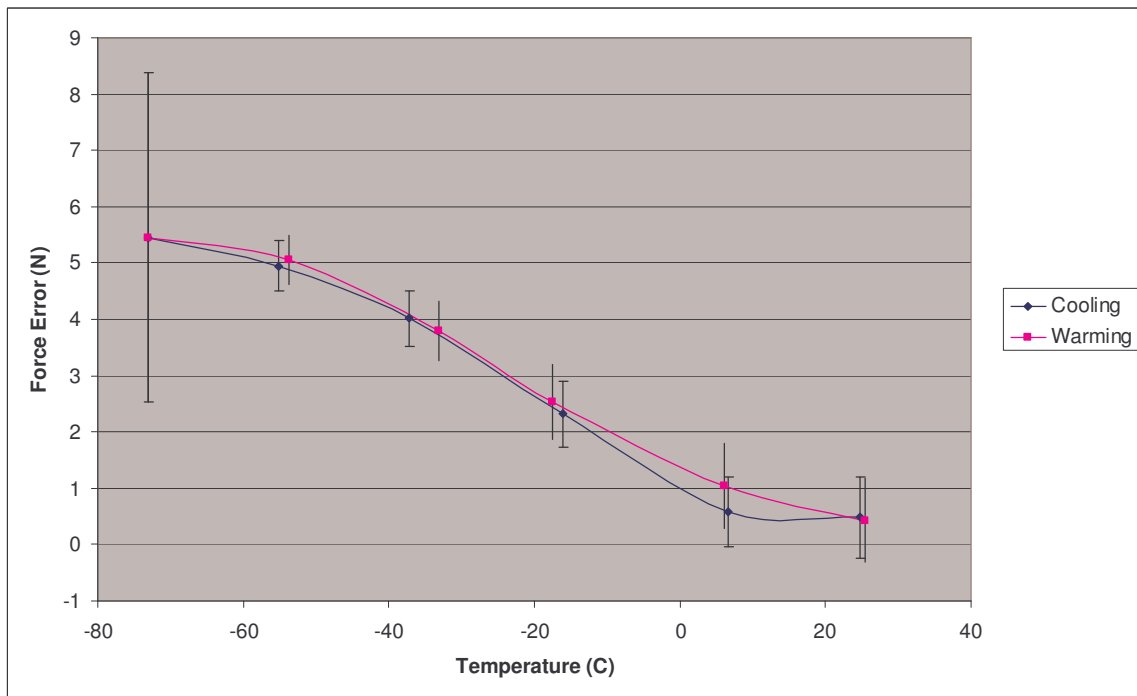


**Figure 26:** Test 2 summary of results

### 4.3 Test 3

Test date: 12/12/2005

Deep cycle #2 performed before this test on 12/9/2005

1 hour at +110°C, 1 hour at -135°C

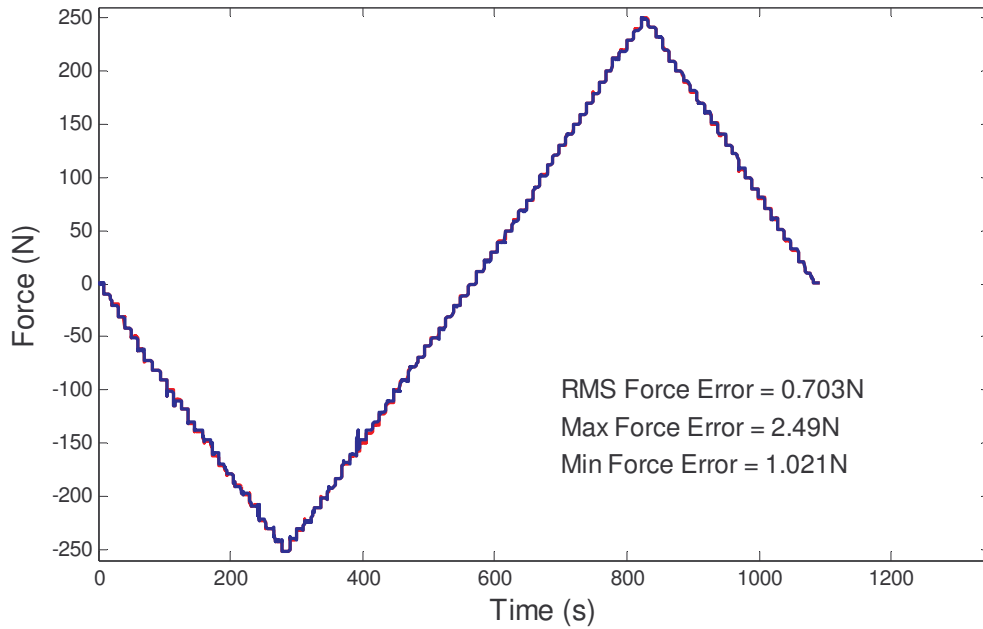


**Figure 27:** Test 3, room temperature (mean 22.2°C, std dev 0.07), cooling

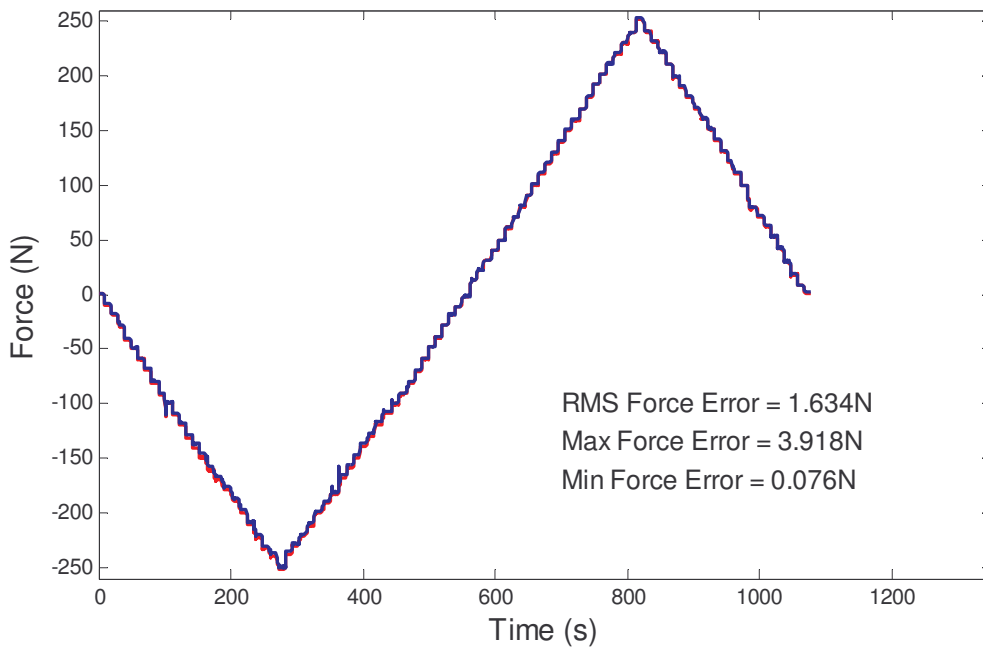


**Figure 28:** Test 3, 5°C (mean 5.2°C, std dev 0.34), cooling

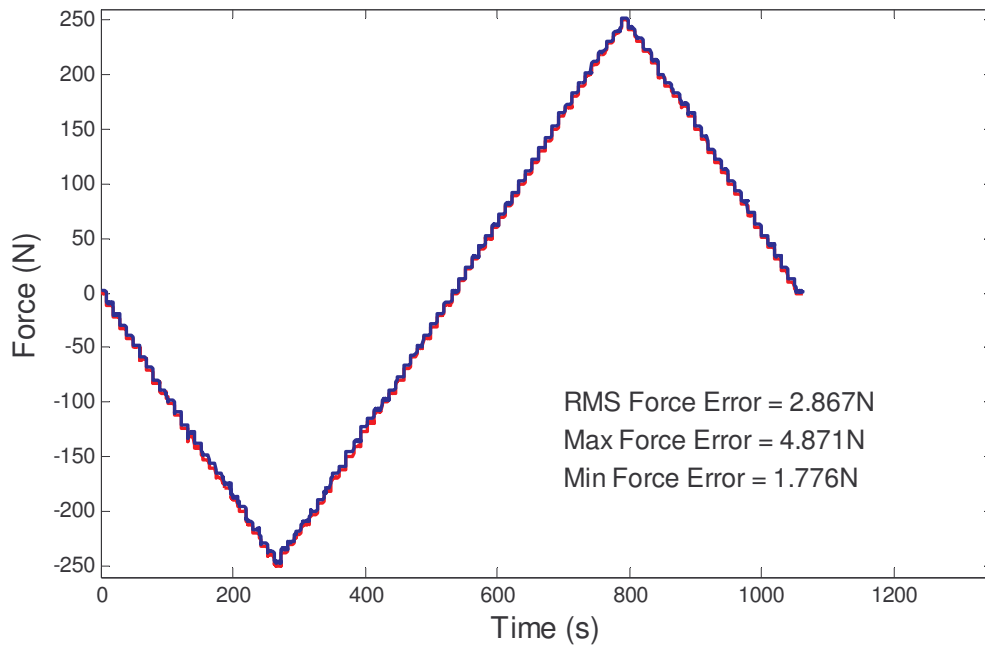


**Figure 29:** Test 3, -15°C (mean -16.2°C, std dev 1.02), cooling

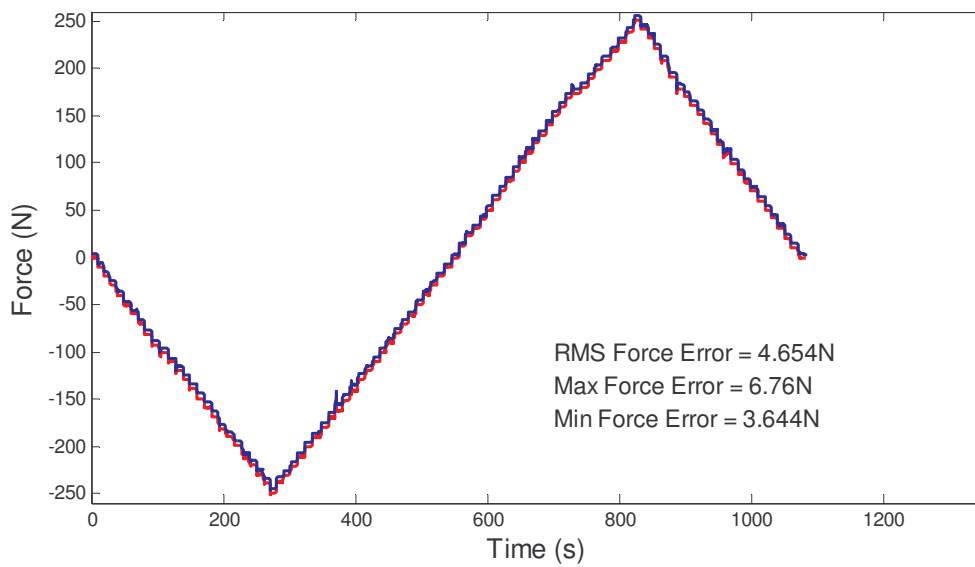


**Figure 30:** Test 3, -35°C (mean -38.7°C, std dev 0.53), cooling

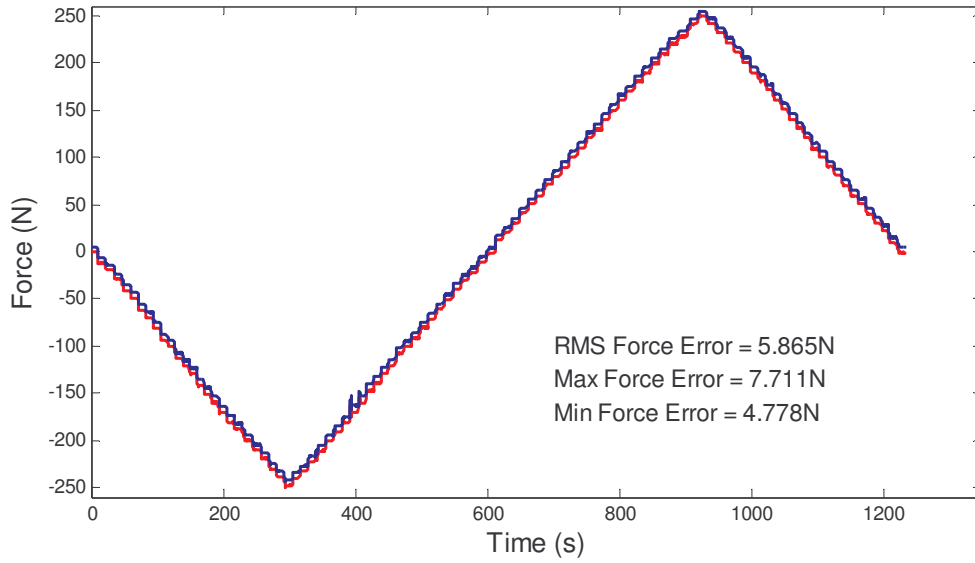


**Figure 31:** Test 3, -55°C (mean -59.4°C, std dev 0.48), cooling

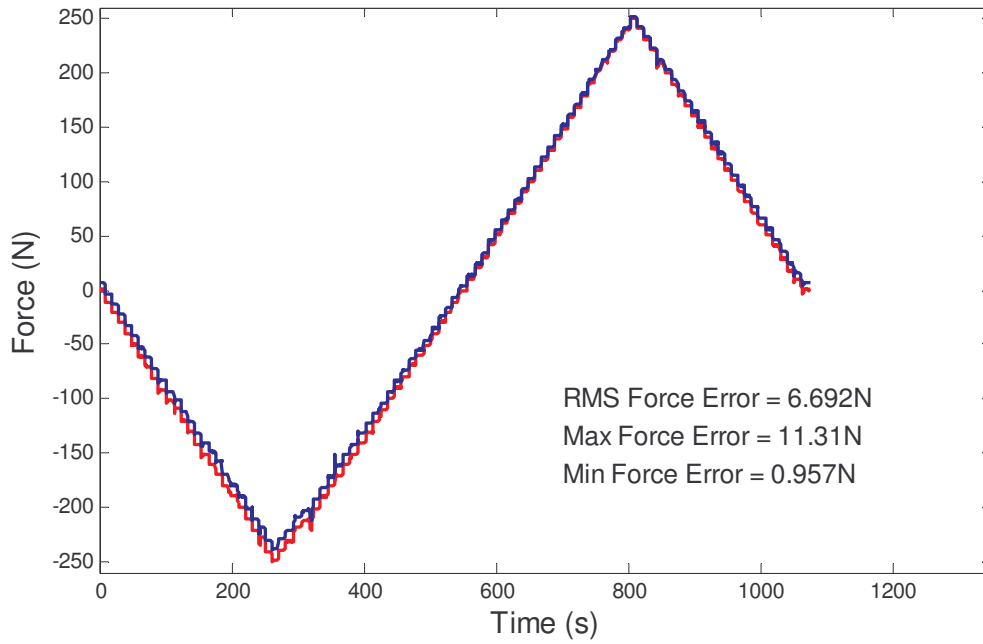


**Figure 32:** Test 3, -70°C (mean -69.2°C, std dev 0.26)

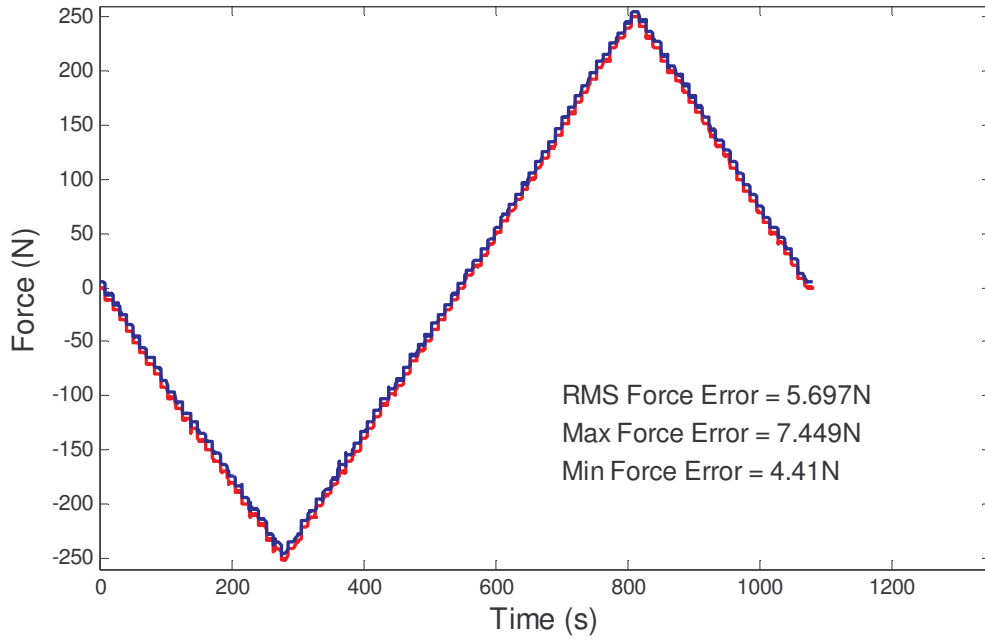


**Figure 33:** Test 3, -55°C (mean -52.9°C, std dev 0.29), warming

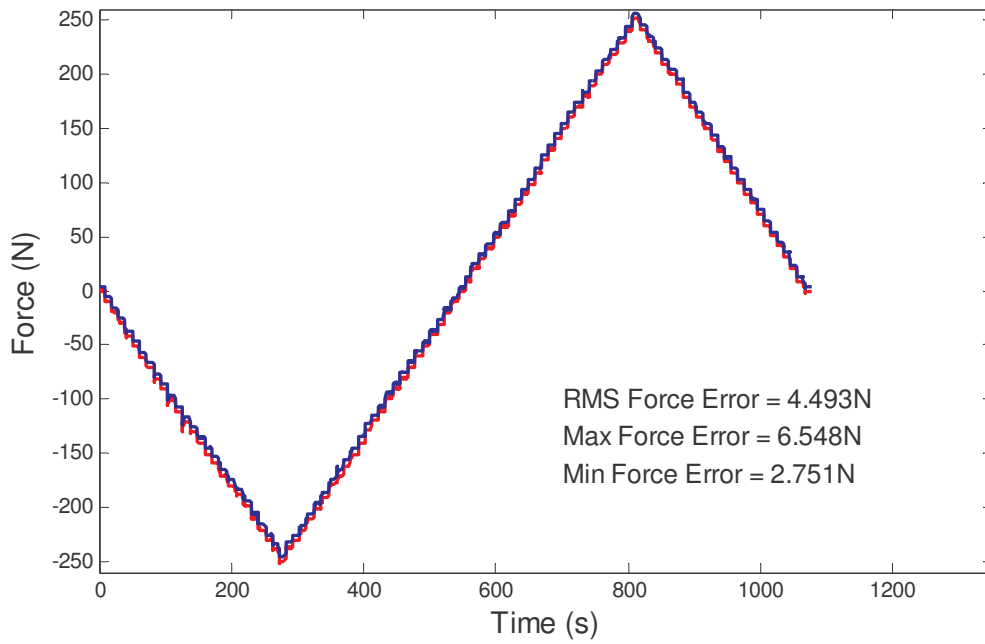


**Figure 34:** Test 3, -35°C (mean -34.3°C, std dev 0.15), warming

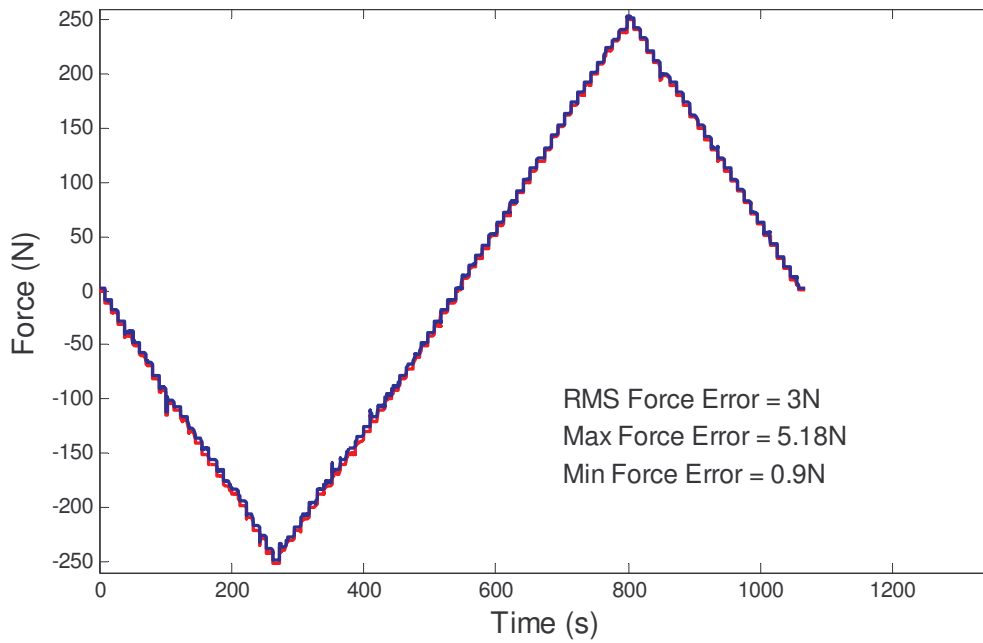


**Figure 35:** Test 3, -15°C (mean -12.7°C, std dev 0.15), warming

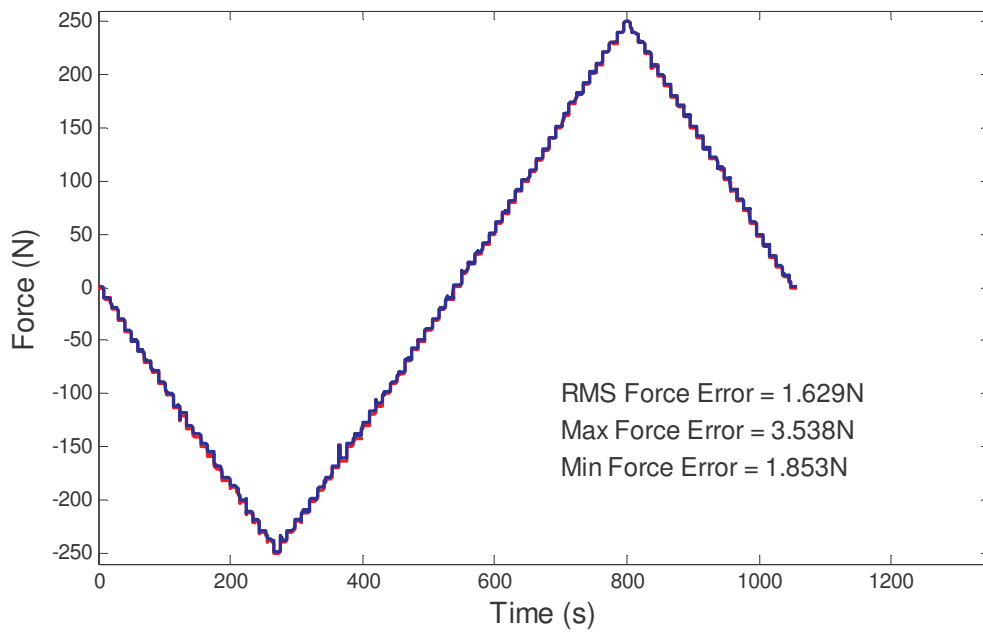


**Figure 36:** Test 3, 5°C (mean 7.1°C, std dev 0.24), warming

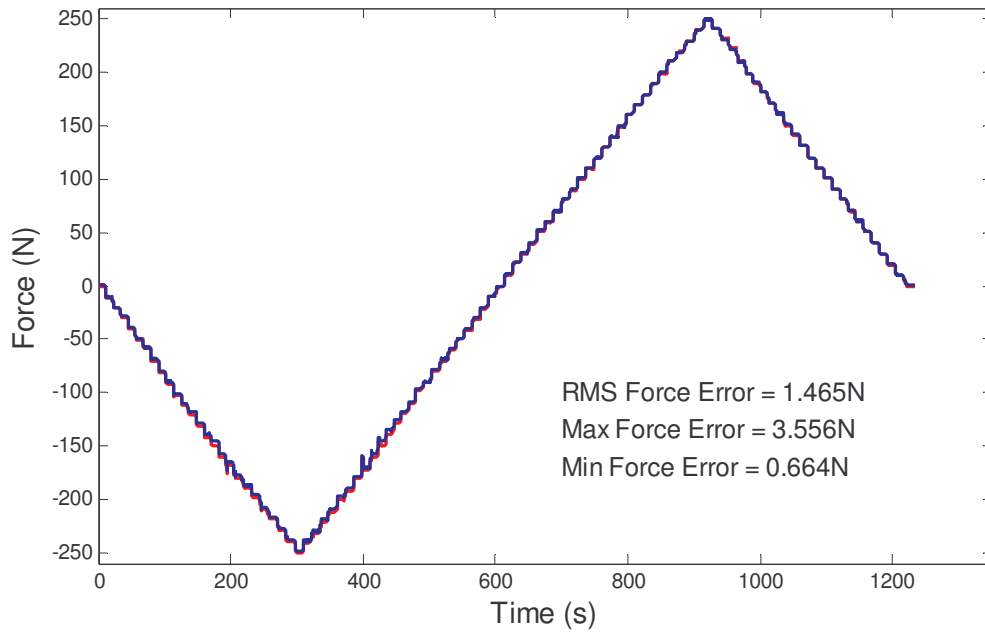


**Figure 37:** Test 3, room temperature (mean 26.6°C, std dev 0.64), warming

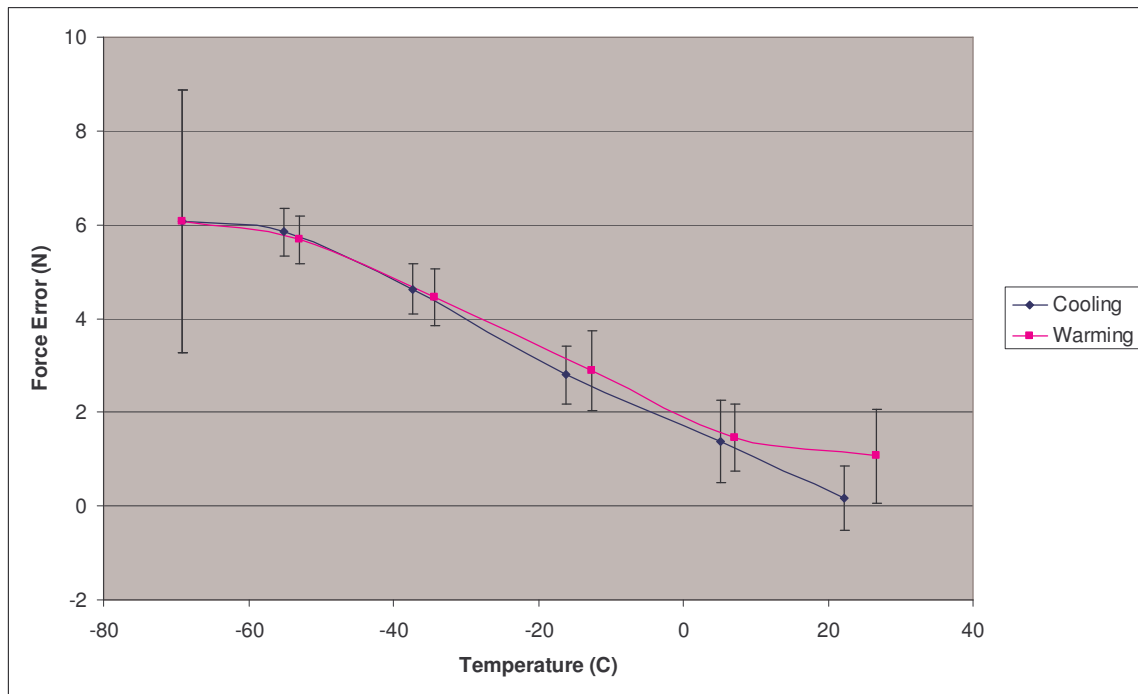


**Figure 38:** Test 3 results summary



## 4.4 Summary

Deep cycle #3 performed on 12/13/2005

1 hour at +110°C, 1 hour at -135°C

Functionality test performed on 12/13/2005: no anomalies

In Figure 39, the mean force error vs. mean temperature from all 33 functional tests are plotted together. They are again separated into cooling and warming categories. The dotted lines represent 3<sup>rd</sup> order polynomial trend line fits of these two categories.

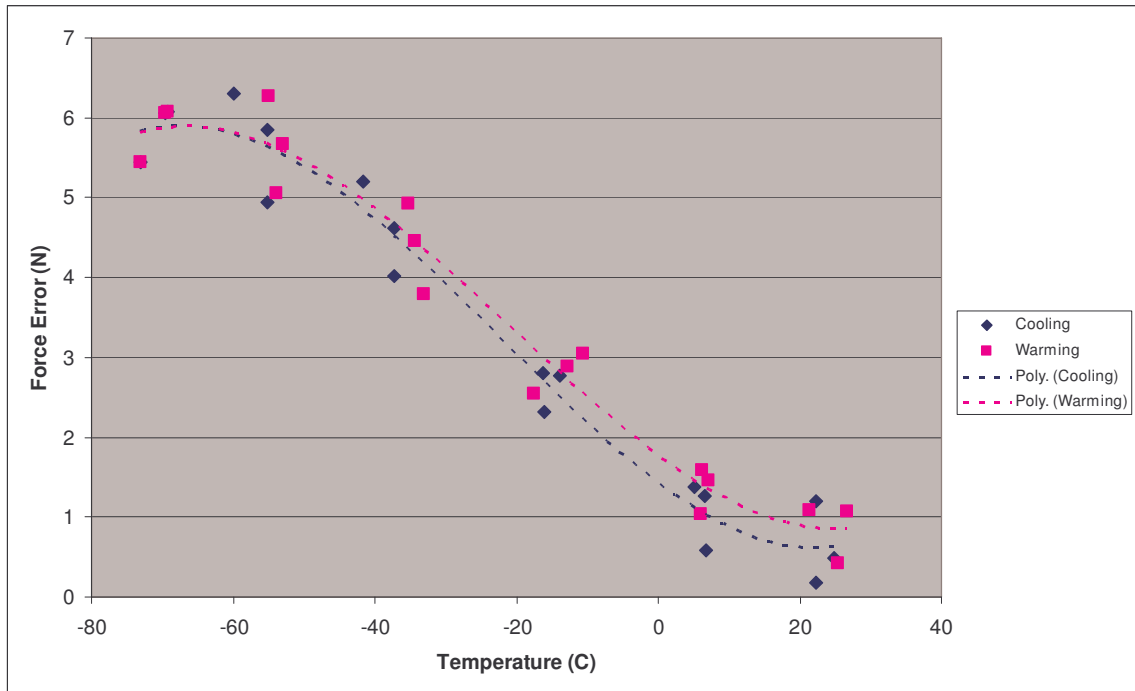


Figure 39: Combined error vs. temperature results

For clarity, the mean error and temperature values calculated for the points in Figure 39 is also tabulated in the following two tables,

Table 1 and Table 2:

**Table 1:** Mean temperature values and deviation for each test

Test 1:		Test 2:		Test 3:	
Temp (°C)	Std Dev (°C)	Temp (°C)	Std Dev (°C)	Temp (°C)	Std Dev (°C)
22.3	0.15	24.8	0.67	22.2	0.07
6.6	0.1	6.7	0.19	5.2	0.34
-13.9	0.21	-16.1	0.52	-16.2	1.02
-41.6	0.53	-37.3	0.38	-38.7	0.53
-60	0.77	-55.1	0.08	-59.4	0.48
-69.6	0.53	-73.1	0.13	-69.2	0.26
-55	0.09	-53.8	0.2	-52.9	0.29
-35.2	0.96	-33.1	0.16	-34.3	0.15
-10.6	0.28	-17.5	3.04	-12.7	0.15
6.2	0.14	6.1	0.38	7.1	0.24
21.4	0.26	25.4	0.76	26.6	0.64

**Table 2:** Mean force error values and deviation for each test

Temp (°C)	Test 1:		Test 2:		Test 3:	
	Mean Error (N)	Std Dev (N)	Mean Error (N)	Std Dev (N)	Mean Error (N)	Std Dev (N)
23	-1.195	0.985	-0.481	0.724	-0.173	0.682
5	-1.267	0.830	-0.591	0.617	-1.374	0.885
-15	-2.776	0.855	-2.316	0.579	-2.800	0.618
-35	-5.200	0.711	-4.012	0.484	-4.623	0.537
-55	-6.301	0.743	-4.948	0.451	-5.842	0.519
-70	-6.054	2.425	-5.451	2.919	-6.080	2.797
-55	-6.265	0.743	-5.048	0.439	-5.675	0.495
-35	-4.929	0.677	-3.788	0.532	-4.4539	0.594
-15	-3.043	0.796	-2.540	0.666	-2.878	0.850
5	-1.5808	0.723	-1.040	0.755	-1.459	0.724
23	-1.0856	0.749	-0.427	0.744	-1.072	0.999

Figure 40 combines all data from the three days of testing. All tests at a given temperature were combined and the mean force error and mean temperature was calculated. The standard deviation on force error was also calculated and included as error bars to show the repeatability of the force readings.

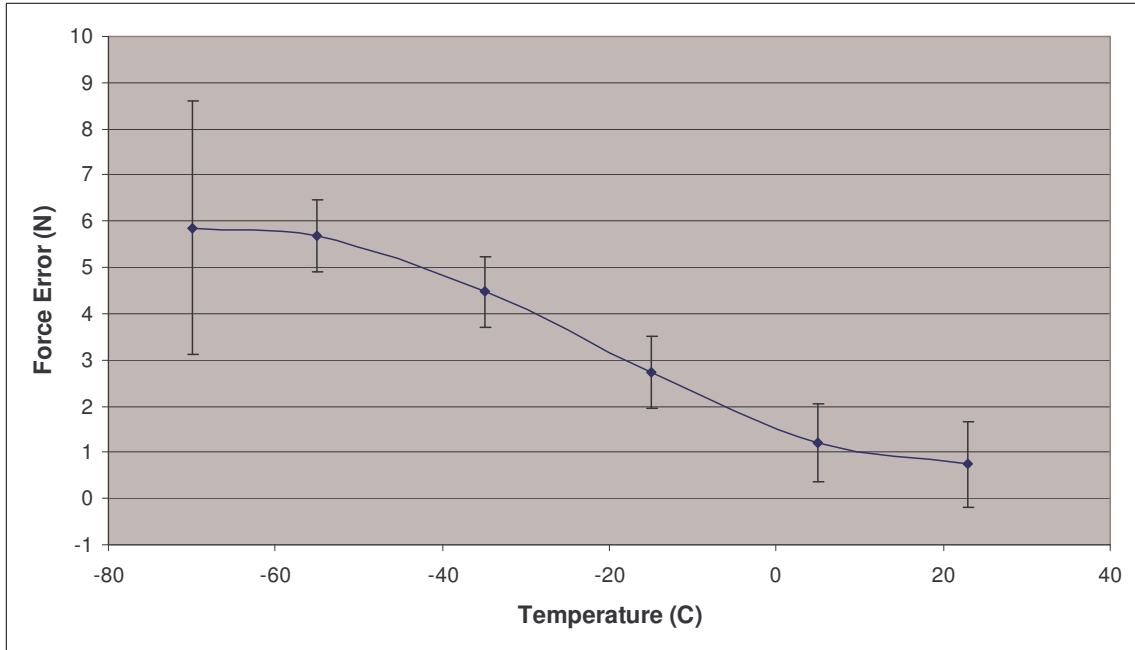


**Figure 40:** Final error vs. temperature calibration with error

In addition to the overall error, it may be useful to know the relationship between force error and applied load. To calculate this, the force error at each data point was divided by the ground truth (from the warm sensor) at that point. Figure 41 shows this relationship by plotting the resulting percent error value against the ground truth force measurement. This was done for each temperature and curves were fit to the data for clarity. The fitted curves are plotted.

Table 3 shows the quality of the curve fits used in Figure 41.

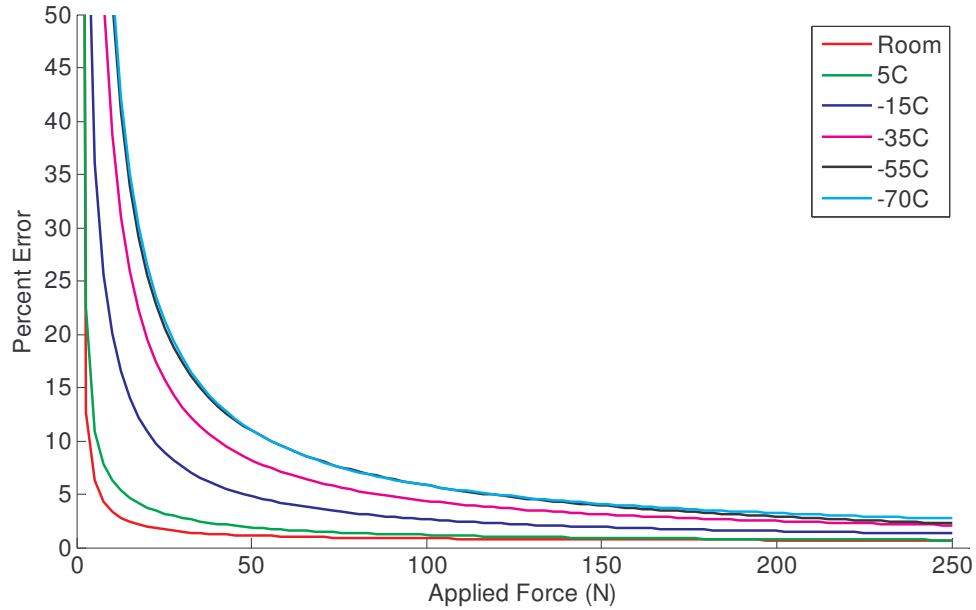


**Figure 41:** Percent error vs. applied force at various temperatures

**Table 3:** Curve fit error and deviation for Figure 41

Temperature (°C)	Mean Error (°C)	Std. Dev. (°C)
23	0.1106	2.801
5	0.1033	2.5066
-15	0.0132	1.3407
-35	0.0144	1.2463
-55	0.0232	1.1857
-70	0.1328	2.9406

## 5 Conclusions

### 5.1 Accuracy

It is apparent from the data that there is a significant temperature dependence despite the temperature compensation circuitry on the cold sensor (see Figure 40 and Figure 41). The sensor exhibits a bias towards tension that is a function of temperature. This has a substantial effect on the accuracy of the sensor. If this sensor were used without knowledge of its current operating temperature then these results show the performance that could be expected for the measurement uncertainty. The mean force error over all trials (for all temperatures and all forces) is 3.21N with a standard deviation of 2.27N. The use of a temperature calibration curve would eliminate this bias and improve force accuracy to that of the sensor's repeatability.

### 5.2 Repeatability

As can be seen in Figure 40, the repeatability of the sensor for all but the -70°C tests is approximately 1N (at one standard deviation). At -70°C, the repeatability begins to degrade and the one standard deviation increases to 2.7N. Using a standard temperature calibration curve (in addition to locally sensing the operational temperature of the sensor), these are the measurement uncertainties that could be achieved with this sensor.

### 5.3 Hysteresis

Plotting the warming and cooling data separately (see Figure 39) reveals a small degree of hysteresis in the error vs. temperature relationship. On average, the room temperature force reading at the conclusion of each test was about 0.25N higher than the room temperature reading at the start of the test. This deviation is very small and is well within the normal error range on the force sensor and can safely be ignored.

### 5.4 Functionality

The cryogenic sensor continued to function consistently and deterministically throughout all of the tests performed on it. It is not possible to draw any thermal fatigue conclusions from the three functional temperature cycle tests plus the three deep thermal cycle tests, but these tests significantly reduce the risk of using a force sensor on a flight project by proving that this design can work at Mars ambient temperatures. *Appendix A* includes a discussion of a post-test x-ray analysis done on the sensor. No degradation was detected using this method.

### 5.5 Impact on Flight Operations

Because the most likely range of operation of this sensor will be 50 to 100N, it is useful to assess the force error in this range. With no additional temperature calibration, the 3.2N (with a 2.3N standard deviation) force error corresponds to 6.4% of the applied load at 50N. Including one standard deviation, this force error encompasses a range of 1.9%-11.0%

Incorporating a compensation scheme as discussed in Section 5.2 would require the measurement of temperature close to the force sensor. If this is included, however, the force error at 50N would be improved to 1.6% (for one standard deviation) above -70°C.

## Appendix A – Post-test Hardware Analysis

Using a Fein x-ray machine, the force sensor used in the experiment was examined alongside an identical, unused sensor. The internal structure was observed to have 4 legs, extending radially at 90° increments to connect a central structure to the outer housing. Each of these four legs was observed to have multiple bonding sites for strain gages. Additionally, there were two areas on the sides of the sensor and one area by the wiring connector where additional strain gauges were mounted, most likely for the temperature compensation circuitry.

The resolution and contrast of the x-ray images were not high enough to make out specific features of the strain gauges or their bonding sites. It was possible, however, to observe proper wiring to each of the strain gauges and to observe any catastrophic failures where the strain gauge may have completely disconnected.

Included in this appendix are the x-ray images of the two sensors and the 7 strain gauge connection sites (4 legs, 2 temperature compensation sites, and 1 interface site). Images labeled “Cold Sensor” are from the sensor tested in the cryogenic chamber. Images labels “690” are the control sensor. Figure 42 is a diagram of the sensor layout describing the physical location of each of the images.

There is no discernable difference between the two sets of images indicating that the cold sensor appears undamaged. There are connection wires at every strain gauge sites and no strain gauges appear in unexpected locations (after a possible disconnection).

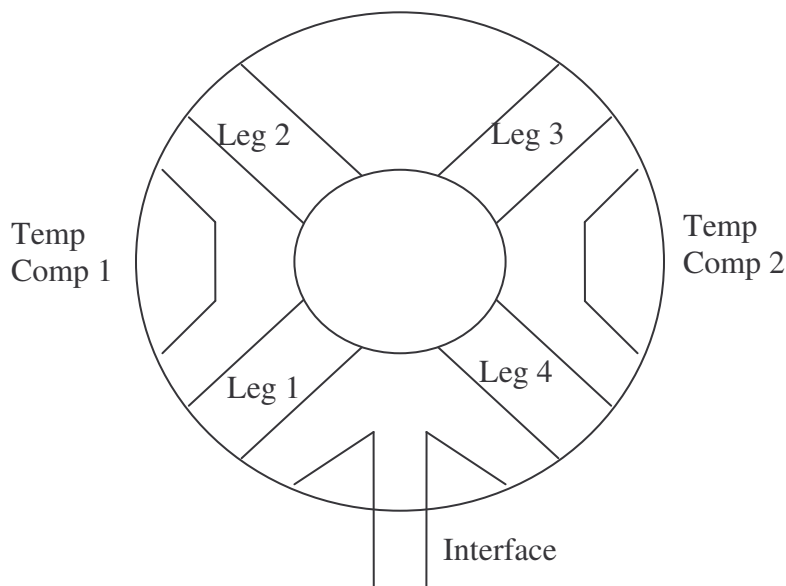
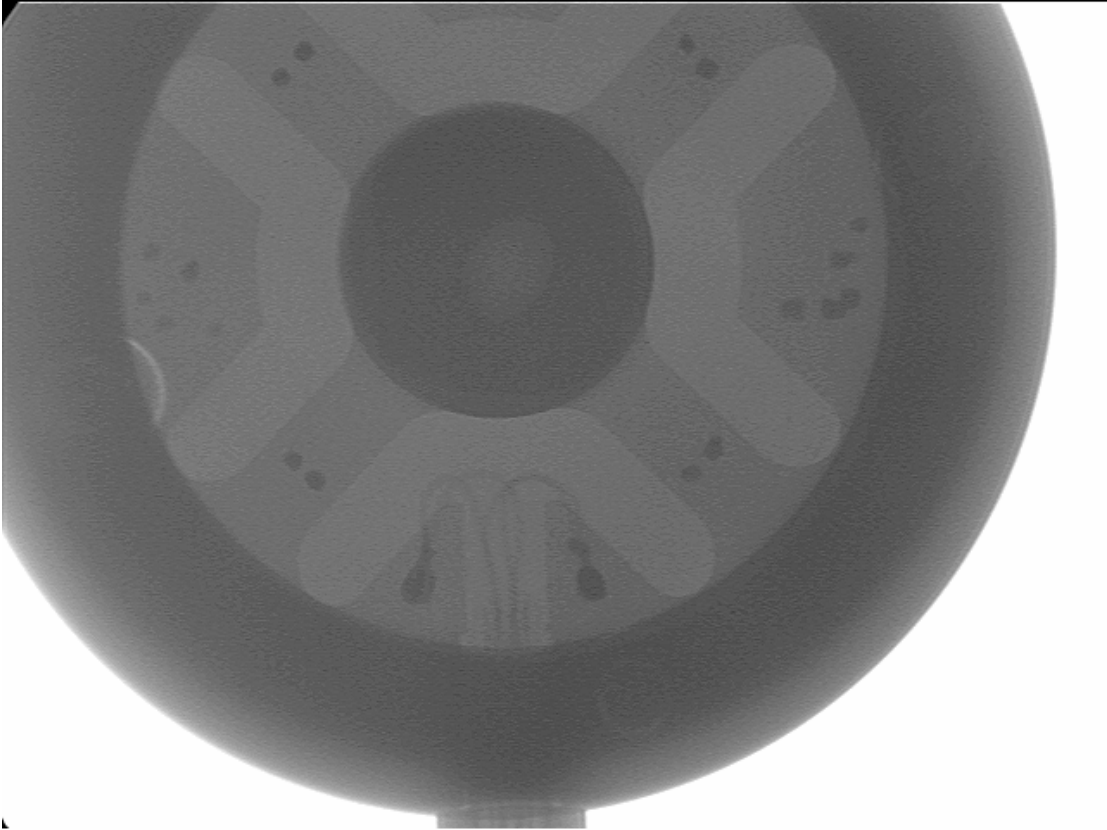
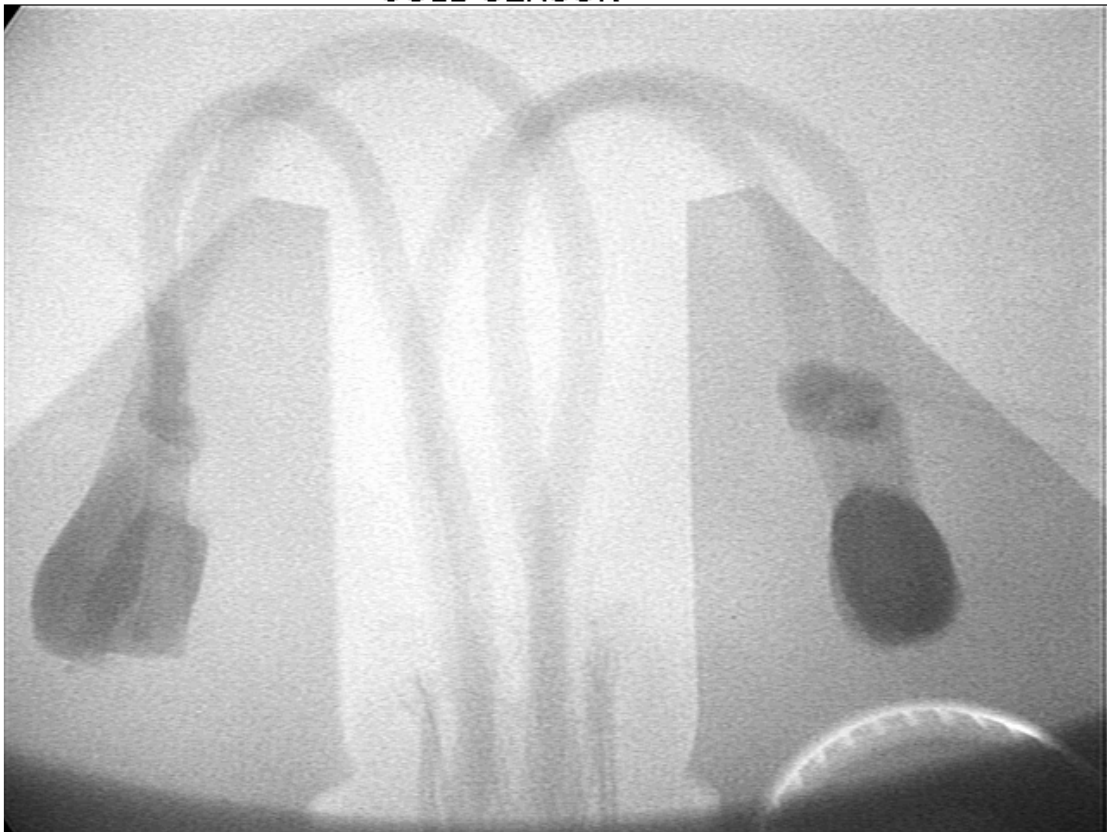


**Figure 42:** Force sensor internal structure with labels

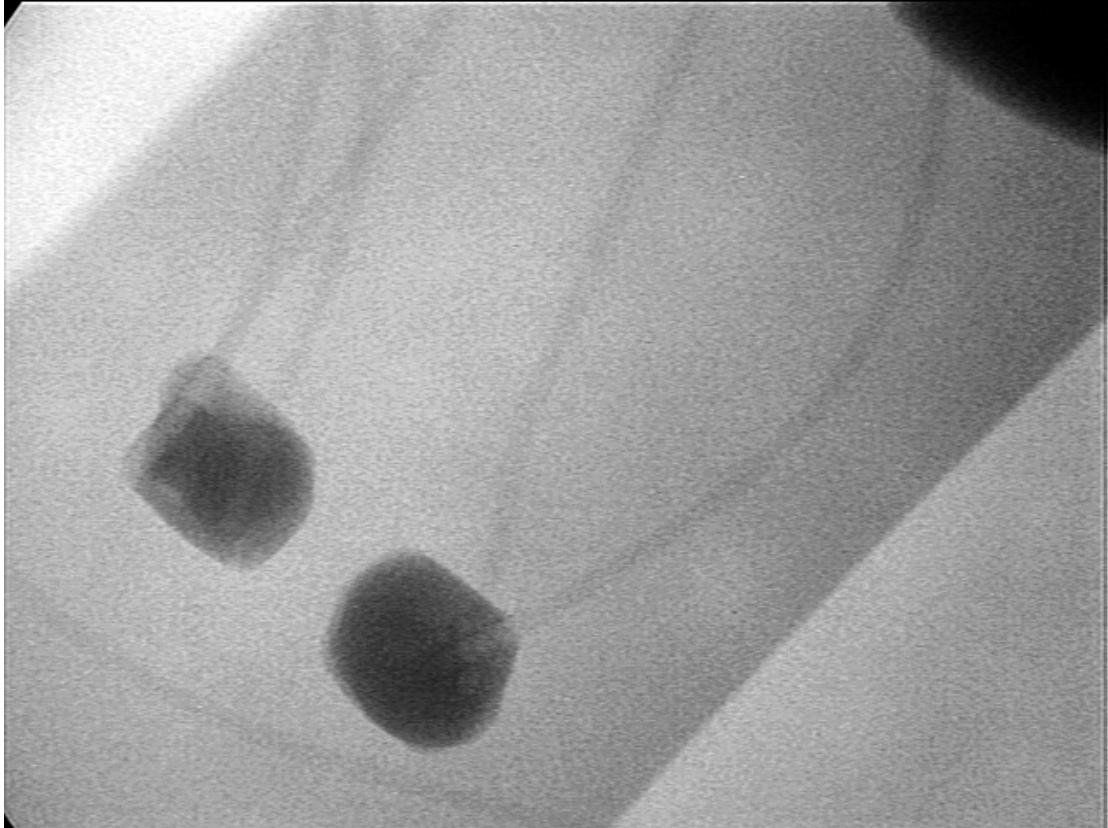


COLD SENSOR

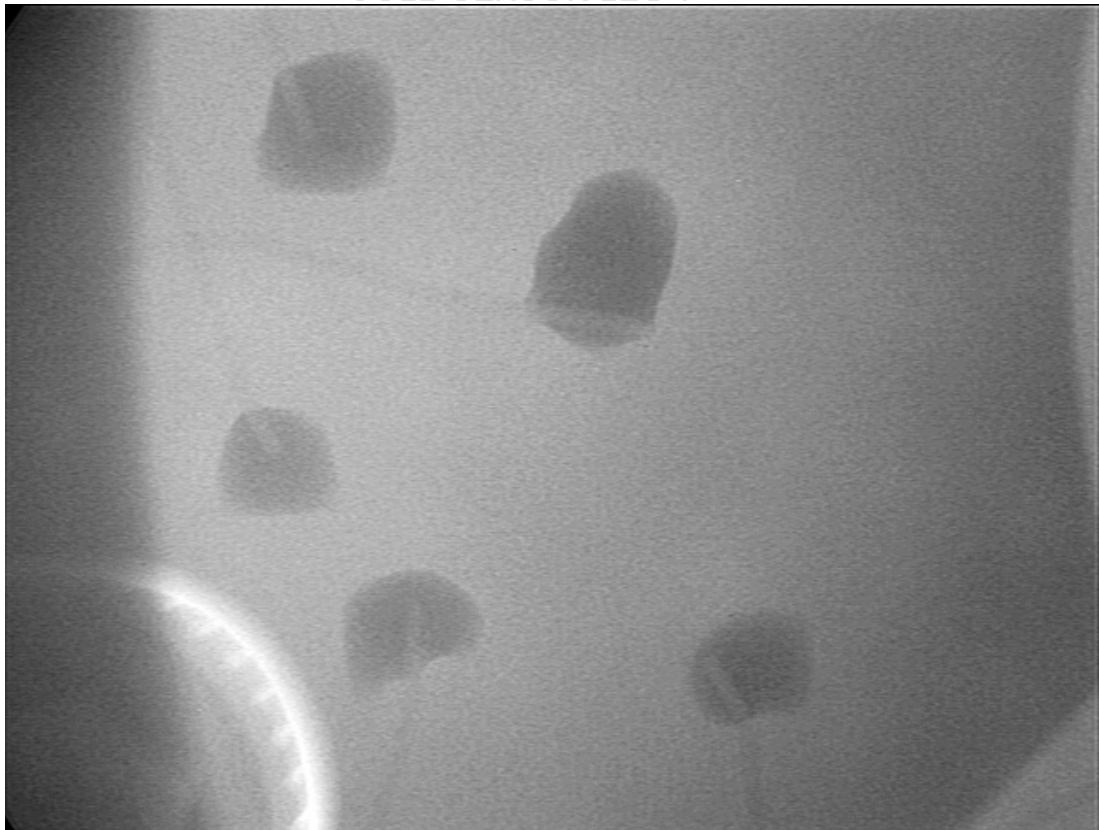


COLD SENSOR INTERFACE

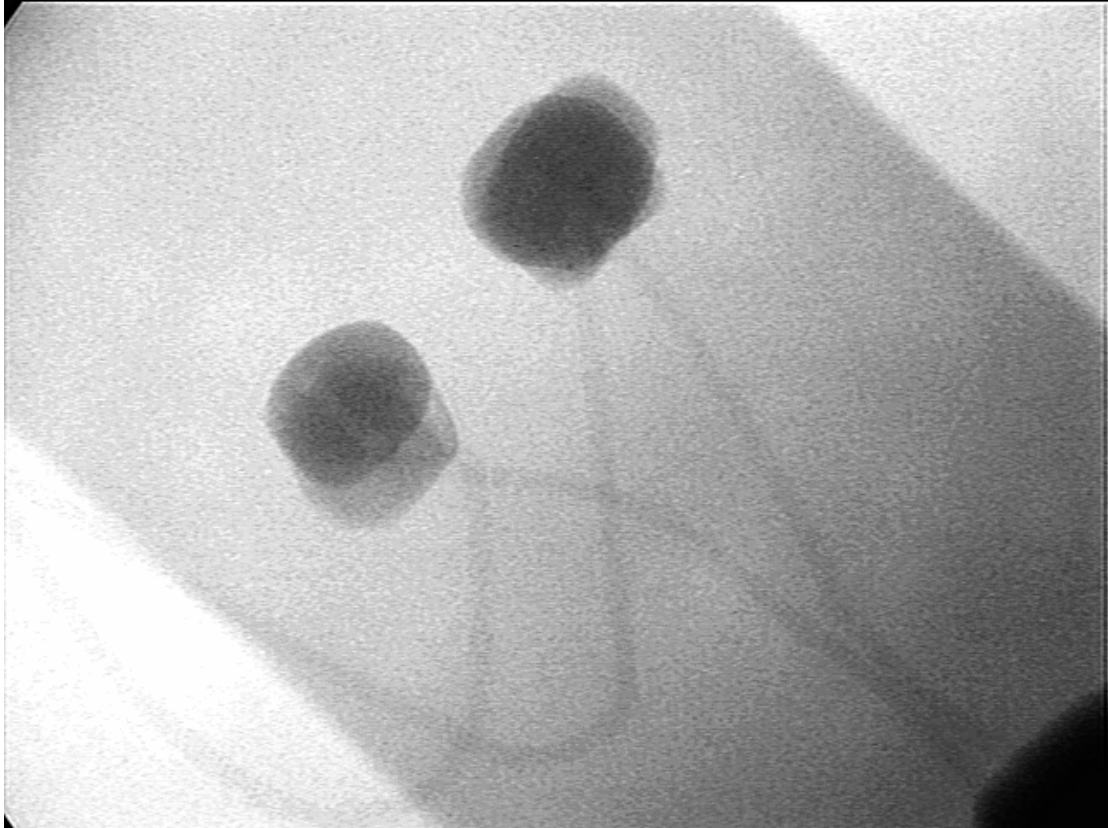




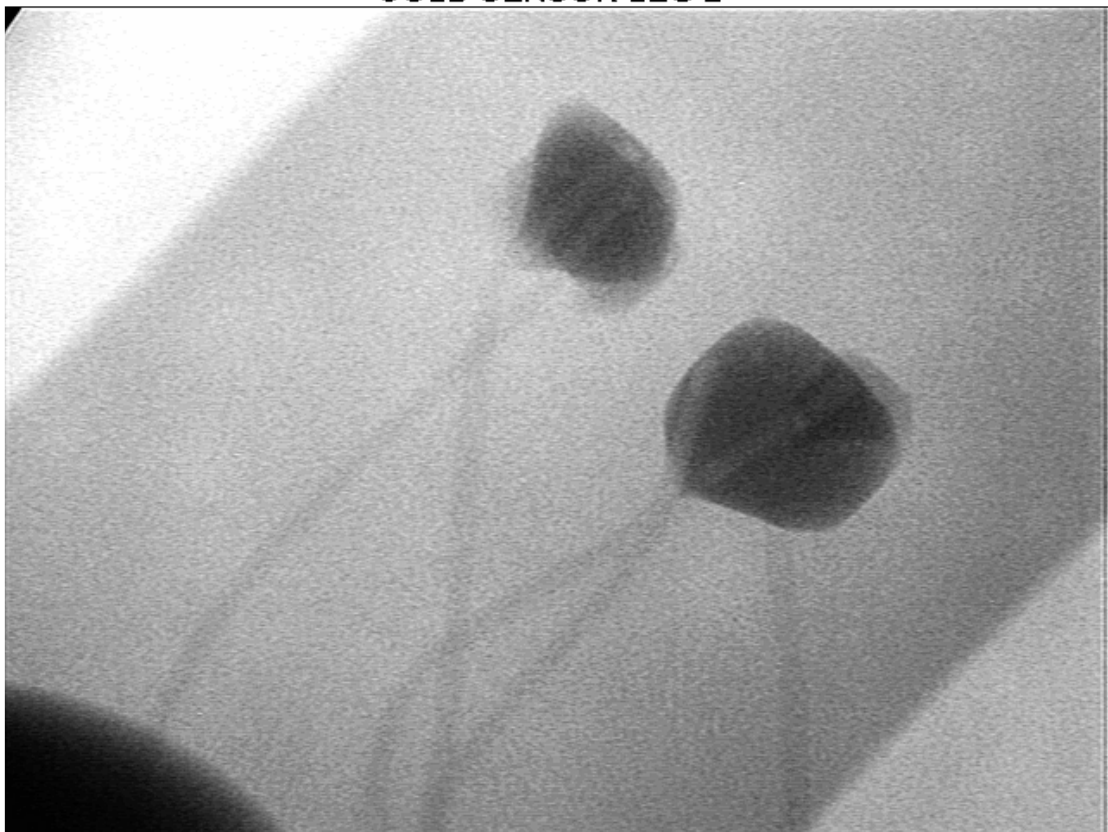
COLD SENSOR LEG 1



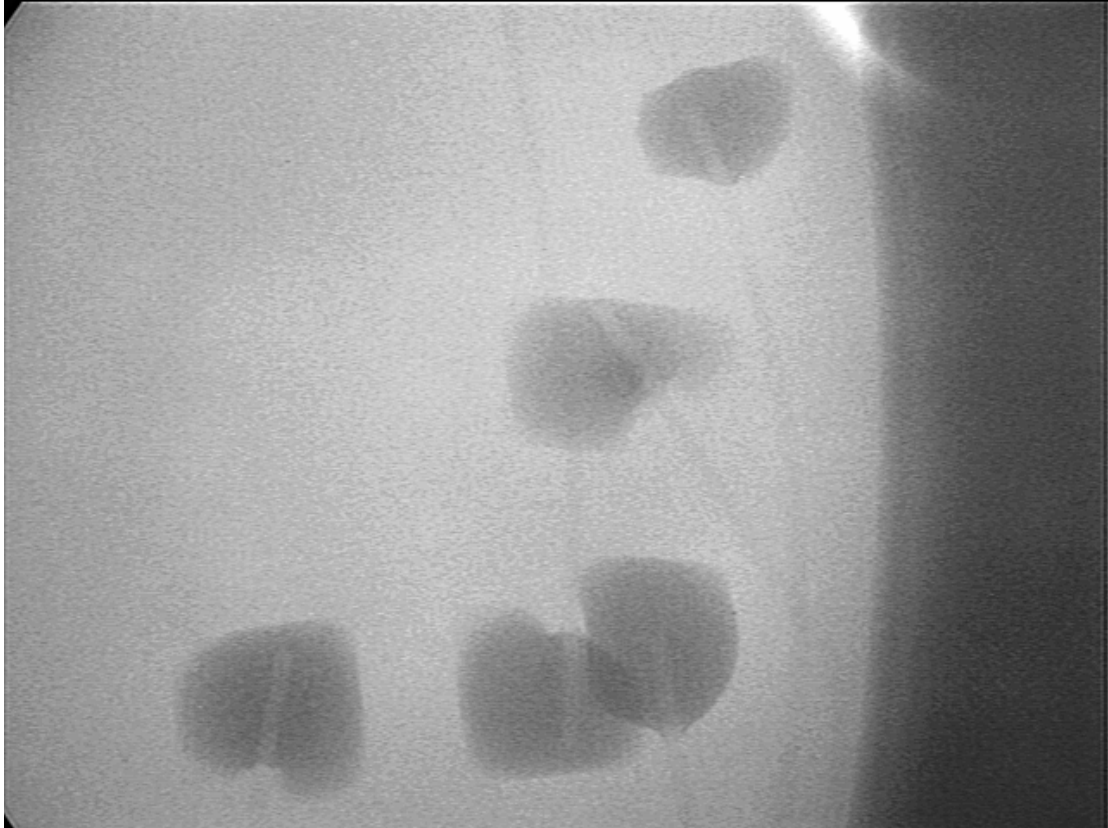
COLD SENSOR TEMP COMP 1



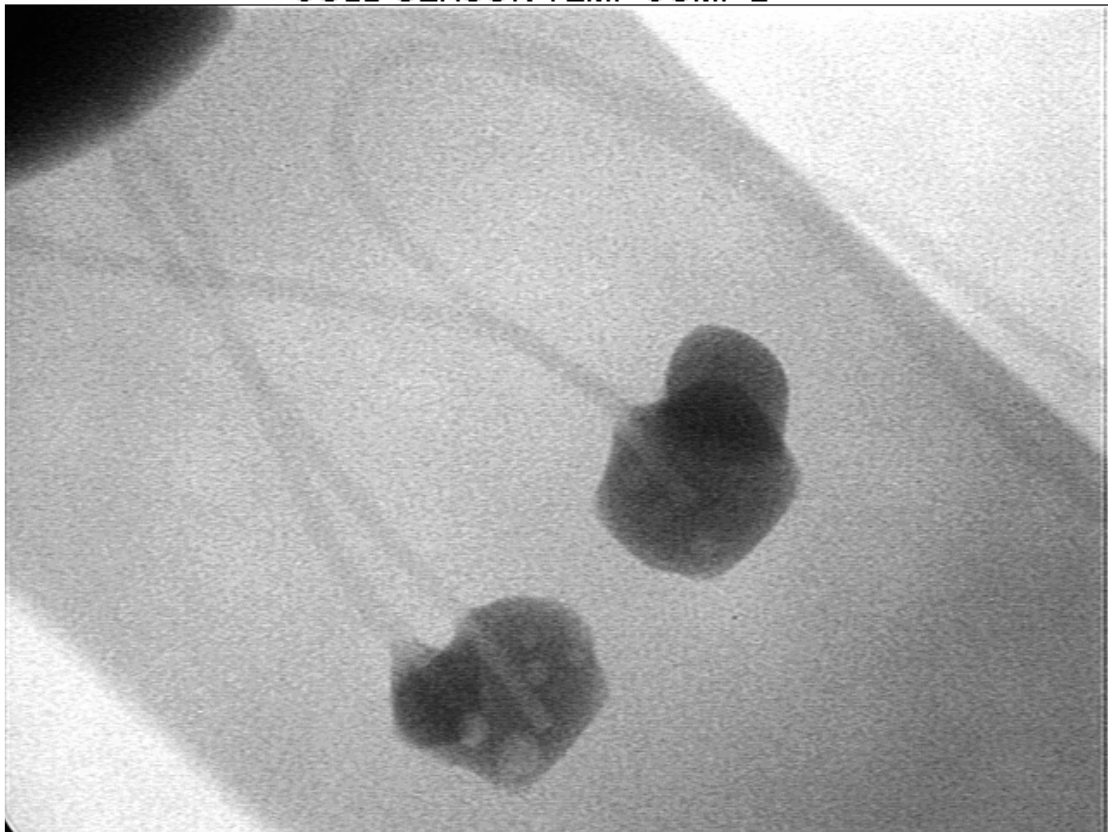
COLD SENSOR LEG 2



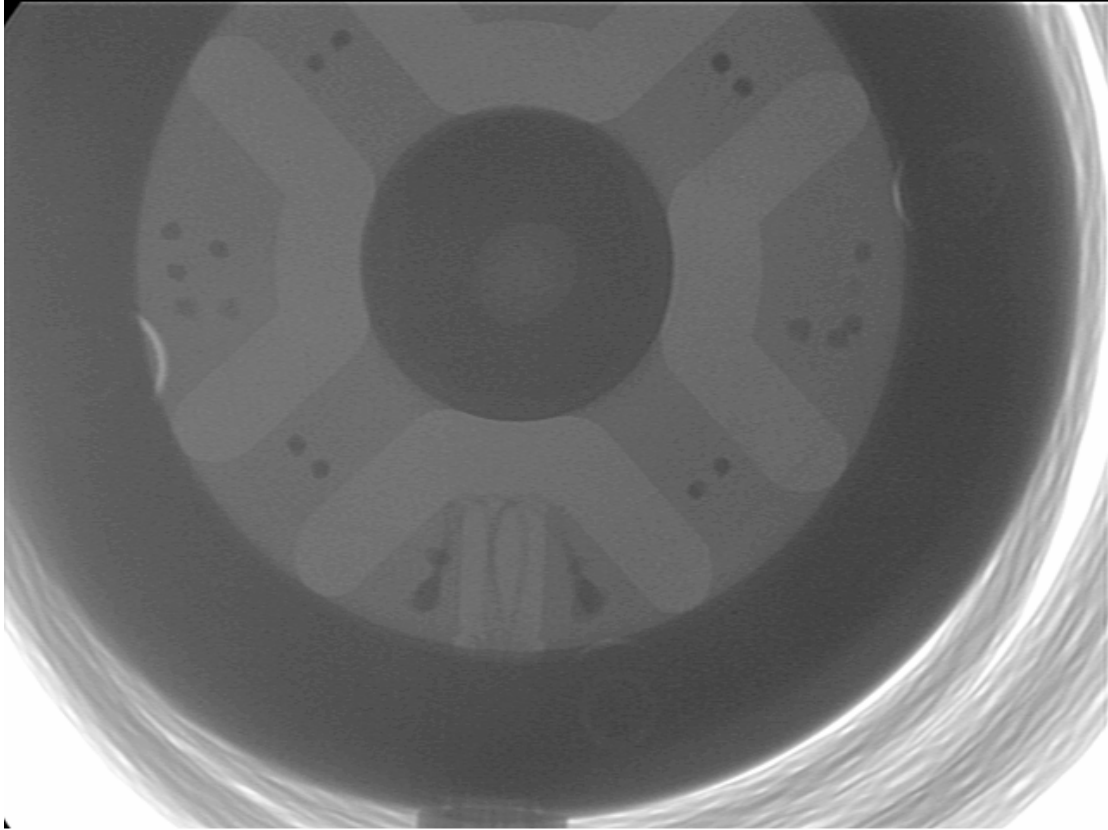
COLD SENSOR LEG 3



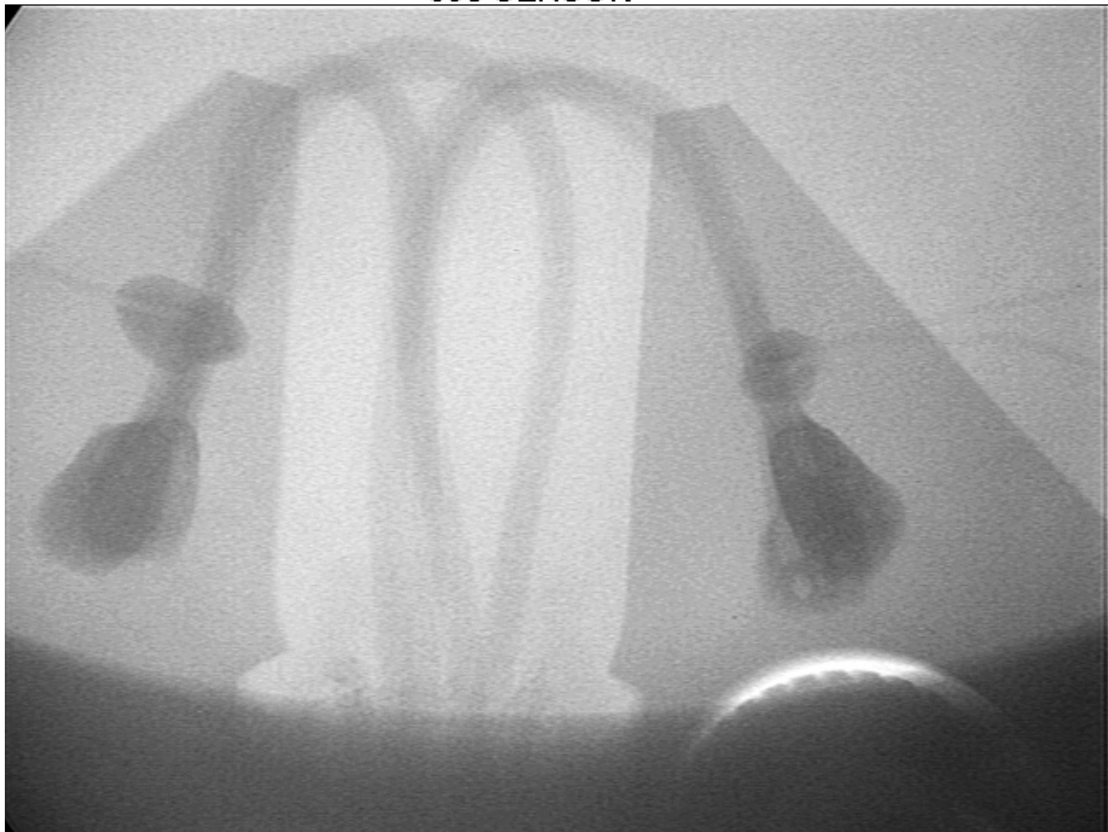
COLD SENSOR TEMP COMP 2



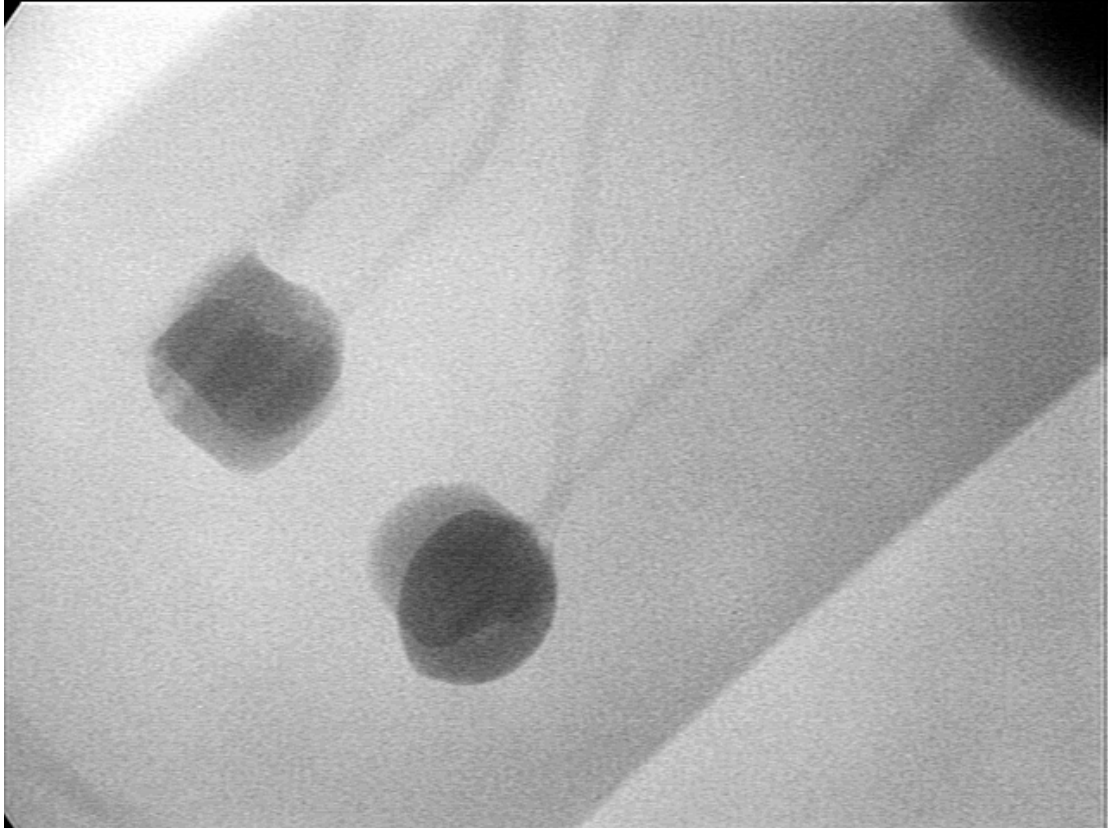
COLD SENSOR LEG 4



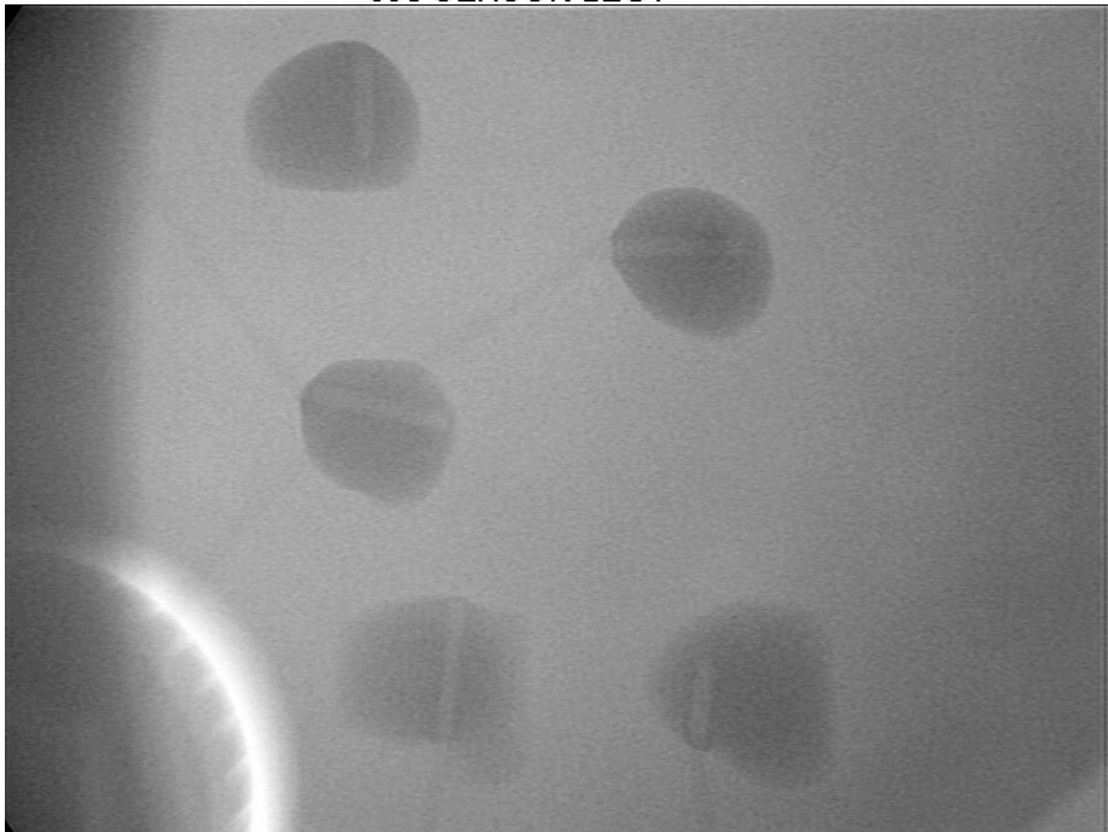
690 SENSOR



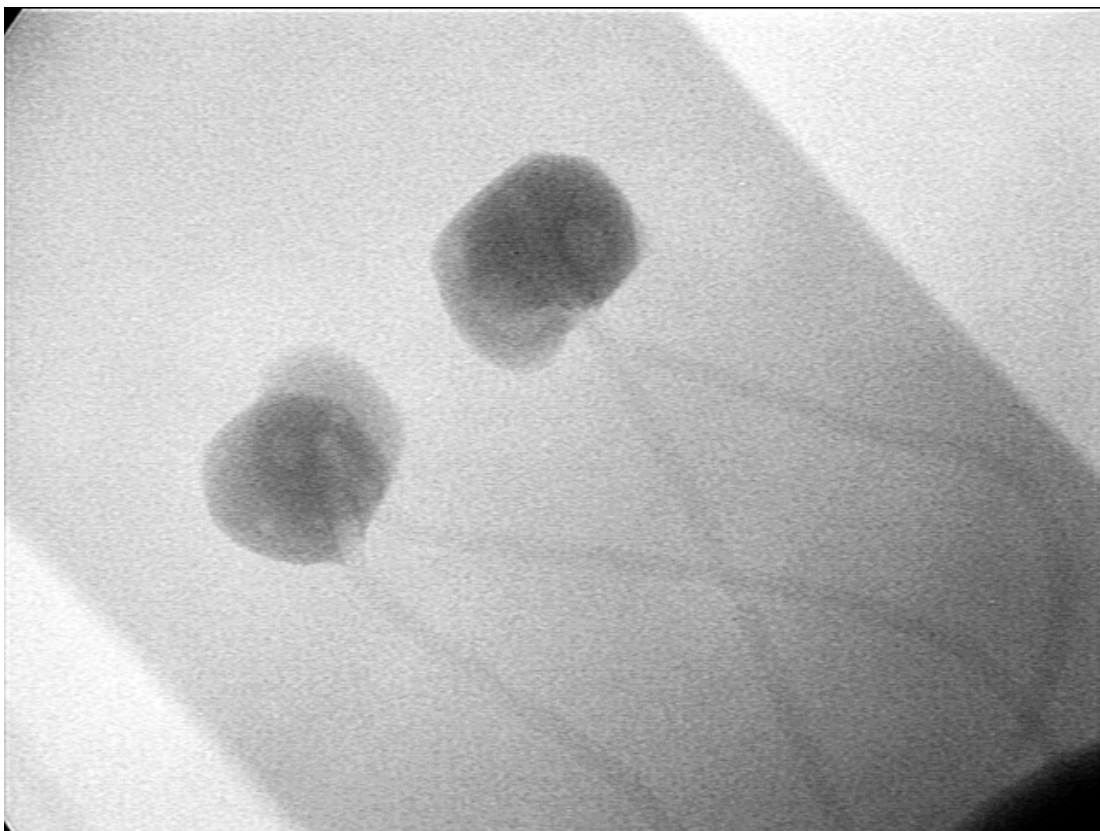
690 SENSOR INTERFACE



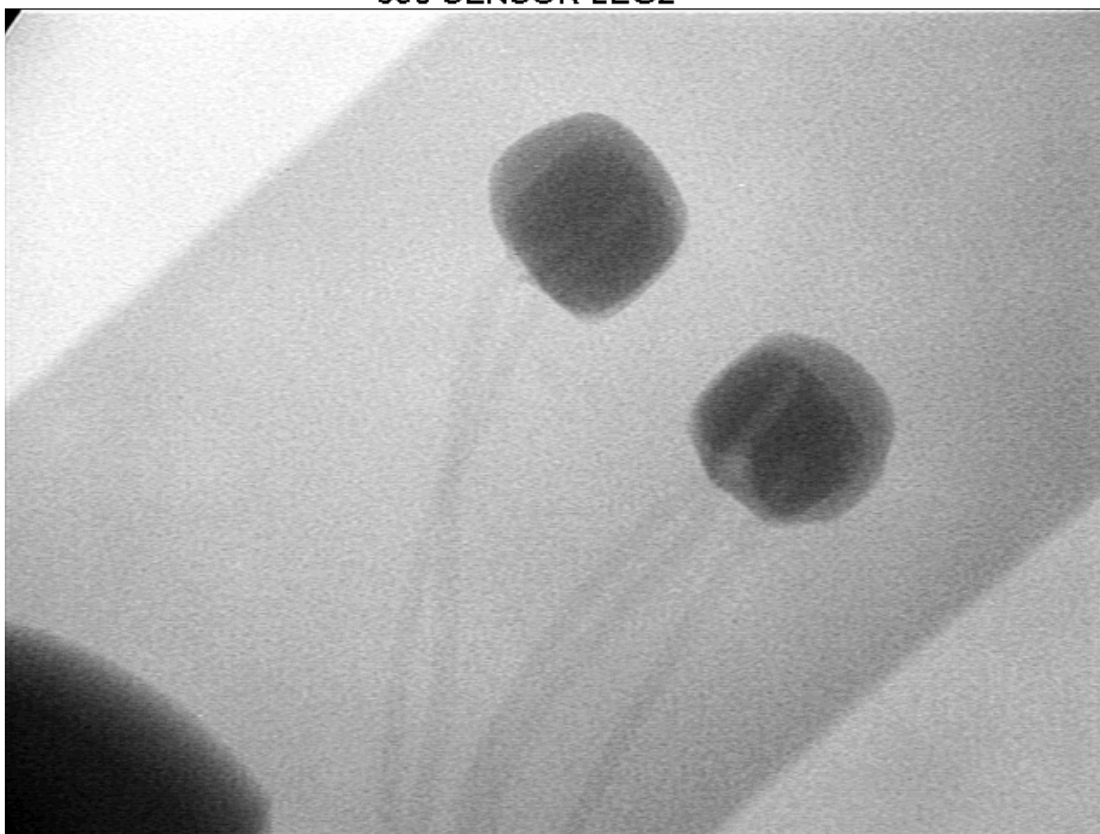
690 SENSOR LEG1



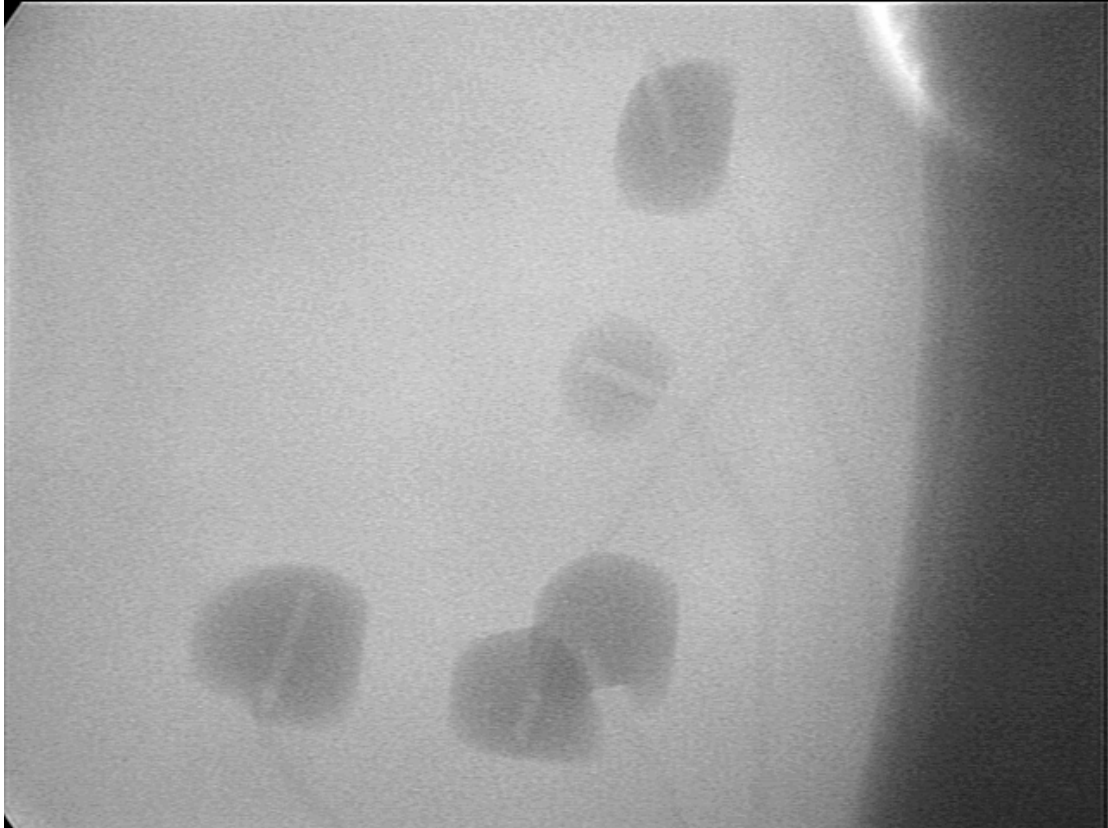
690 SENSOR TEMP COMP1



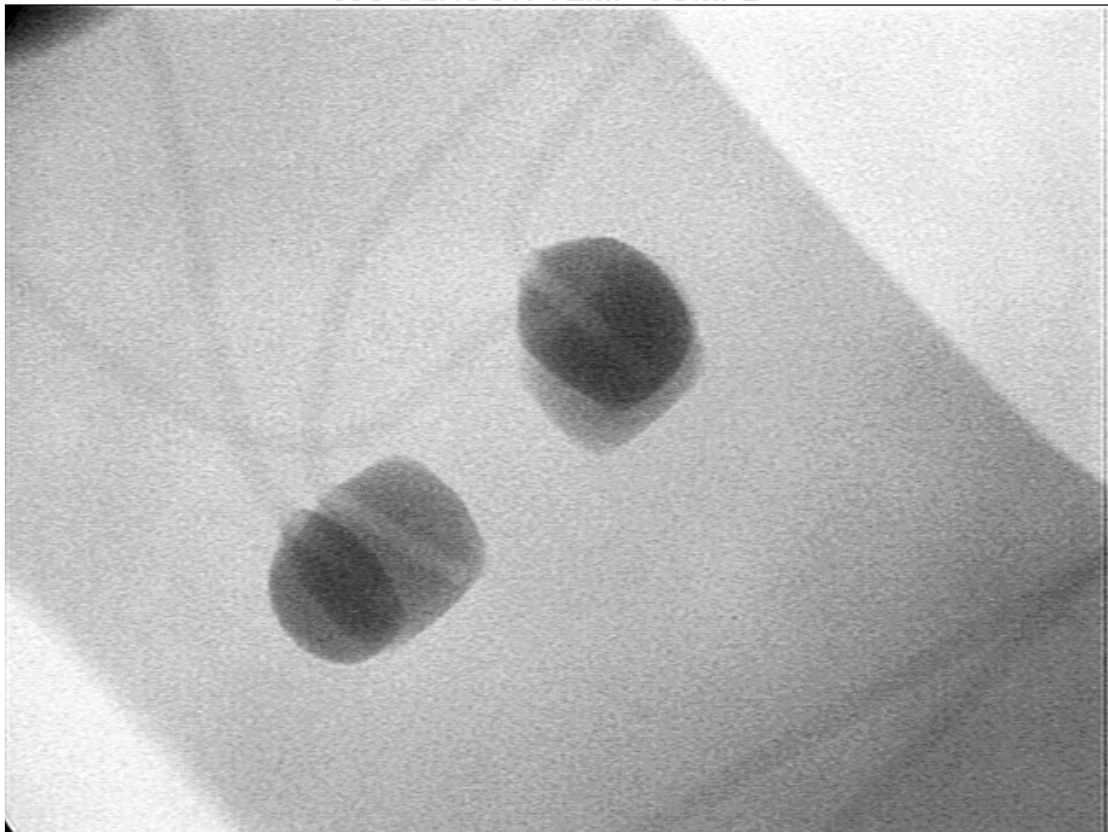
690 SENSOR LEG2



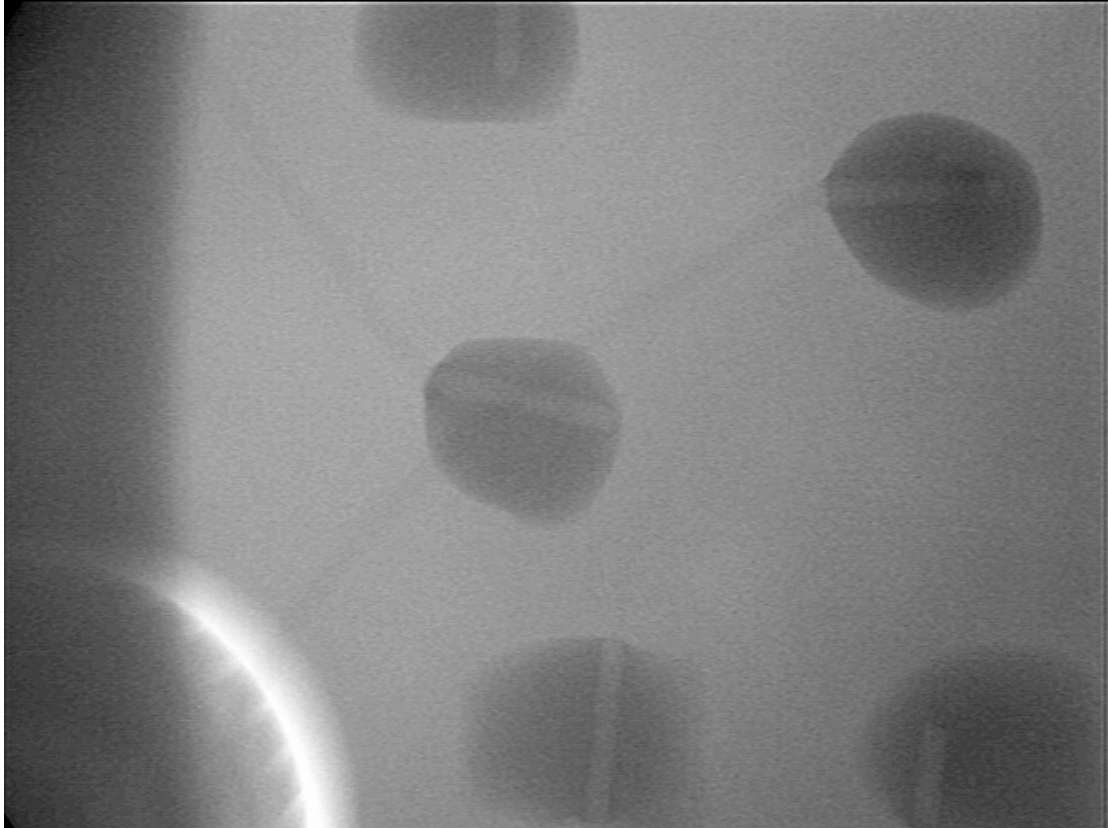
690 SENSOR LEG3



690 SENSOR TEMP COMP2



690 SENSOR LEG4



690 SENSOR TEMP COMP1 CLOSEUP



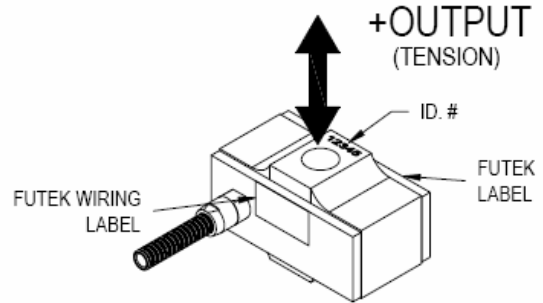
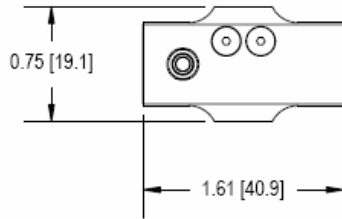
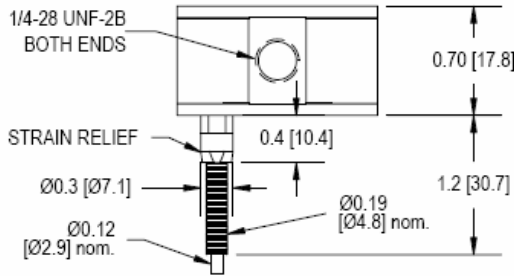
# Appendix B – Warm Sensor Data Sheet

## FUTEK MODEL LRF325 (L2320) *LOW PROFILE TENSION AND COMPRESSION LOAD CELL*

**Drawing Number: FI1069**

**INCH [mm] | R.O.= Rated Output**

WIRING CODE (WC)			
+Excitation	-Excitation	+Signal	-Signal
RED	BLACK	GREEN	WHITE



STK#	CAPACITY	
	lb	N
FSH00073	25	111
FSH00074	50	222
FSH00075	75	334
FSH00076	100	445

**SPECIFICATIONS:**

<b>RATED OUTPUT</b>	2 mV/V nom.
<b>SAFE OVERLOAD</b>	150% of R.O.
<b>ZERO BALANCE</b>	±1% of R.O.
<b>EXCITATION (VDC OR VAC)</b>	15 MAX
<b>BRIDGE RESISTANCE</b>	350 Ω nom.
<b>NONLINEARITY</b>	±0.1% of R.O.
<b>HYSTERESIS</b>	±0.1% of R.O.
<b>NONREPEATABILITY</b>	±0.05% of R.O.
<b>CREEP</b>	±0.05% of LOAD
<b>TEMP. SHIFT ZERO</b>	±0.005% of R.O./°F [0.01% of R.O./°C]
<b>TEMP. SHIFT SPAN</b>	±0.005% of LOAD/°F [0.01% of LOAD/°C]
<b>COMPENSATED TEMP.</b>	60 to 160°F [15 to 72°C]
<b>OPERATING TEMP.</b>	-80 to 200°F [-50 to 93°C]
<b>WEIGHT</b>	1.8oz [51g]
<b>MATERIAL</b>	ALUMINUM
<b>DEFLECTION</b>	0.003 to 0.006 [0.08 to 0.15] nom.
CABLE: #28 AWG, 4 Conductor, Spiral Shielded Clear PVC Cable 10 ft [3 m] Long	
ACCESSORIES AND RELATED INSTRUMENTS AVAILABLE	
<b>CALIBRATION (STD)</b>	5 pt. TENSION; 60.4 KΩ SHUNT CAL. VALUE
<b>CALIBRATION (AVAILABLE)</b>	COMPRESSION
<b>CALIBRATION TEST EXCITATION</b>	10 VDC

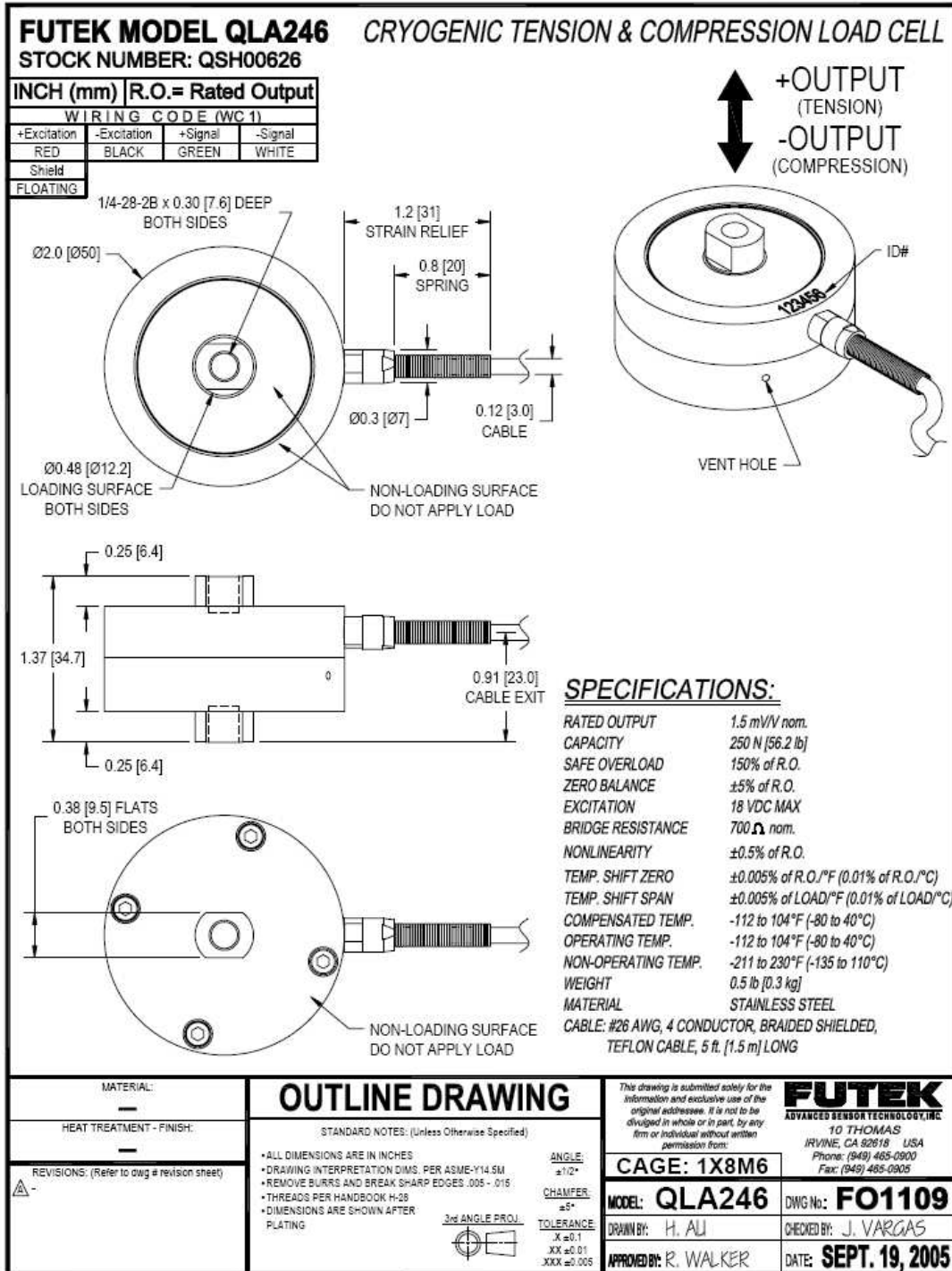
**FUTEK**  
ADVANCED SENSOR TECHNOLOGY, INC.

This drawing is submitted solely for the information and exclusive use of the original addressee. It is not to be divulged in whole or in part, by any firm or individual without written permission from FUTEK

10 THOMAS  
IRVINE, CA 92618 USA  
1-800-23-FUTEK (38835)

INTERNET:  
<http://www.futek.com>

# Appendix C – Cold Sensor Data Sheet



# Appendix D – Warm Sensor Calibration Certificate

## Certificate of Calibration

**FUTEK**  
Advanced Sensor Technology

Certificate Number..... 0508290005

Sensor

Model Number ..... LRF325  
ID Number ..... 48281

Stock No ..... FSH00075  
Capacity ..... 75 lb

Model: LRF325 - 75 lb (L2320)  
Low Profile Tension & Compression  
Ver.1 - Standard  
Aluminum 1/4-28 Thread Standard  
28 Awg 4 Conductor Braided Shielded Clear PVC -

Instrument ID:

Customer Name ..... Jet Propulsion Lab  
Customer Address ..... 4800 Oak Grove Dr, Pasadena CA 91109  
P.O. Number ..... PCARD 1117390055

**REFERENCE CALIBRATION EQUIPMENT**

**Dead Weight:**

Reference NIST Number: MMAP 822/LA M.S. 12372  
System Cal. Date: 02/20/2004 Next Cal. Date by: 02/20/2009

**Digital Indicator:**

HP Model Number: Agilent 34401A S/N: US36134723  
Cal.Date: January 10, 2005 Next Cal.Date by: January 10, 2006  
Uncertainty Value: 0.0050%

This certifies that the following sensor has been calibrated using equipment traceable to NIST in accordance with FUTEK and applicable to the MIL-STD-45662A. Supporting documentation relative to traceability is on file and is available for examination upon request. This certificate shall not be reproduced except in full, without the written approval of FUTEK

Calibrated By: Angel Mendoza  
Shipment Date: Aug. 29, 2005 Re-Calibration Date: One Year After Shipment Date

Certificate Number.....0508290005

**FUTEK**  
Advanced Sensor Technology

**CALIBRATION DATA**

Test Temp ..... 70.00 °F (21.11°C)      Relative Humidity ..... 35.00 %  
 Excitation ..... 10 (Vdc)      Input Resistance ..... 397 (Ohms)  
 Zero ..... -0.0059 (mV/V)      OutPut Resistance ..... 354 (Ohms)

**Tension**

Rated Output ... 2.0424 mV/V      ZeroReturn .... 0.013% of R.O.  
 Linearity ..... 0.057 % of R.O.

**Compression**

Rated Output ... -2.0347 mV/V      ZeroReturn .... -0.044% of R.O.  
 Linearity ..... -0.026 % of R.O.

**DATA POINTS**

Load	Output	Non-Lin Error (%)	Hysteresis (%)
(lb)	(mV/V)		
		<u>Tension</u>	
0	0.0000	0.000	
15	0.4094	0.046	
30	0.8172	0.012	
45	1.2266	0.057	
60	1.6345	0.029	
75	2.0424	0.000	
0	0.0003		

ASTM Uncertainty: 0.00162 mV/V

\* Error and Uncertainty were calculated using Straight Line Method in accordance with ASTM E74 with K = 2

Best Fit Equation:  $Y = A_0 + A_1X + A_2X^2 + A_3X^3$

$A_0 = 1.07938e-004$        $A_2 = -1.65490e-007$

$A_1 = 2.72630e-002$        $A_3 = -3.55617e-009$

Best Fit Equation:  $X = B_0 + B_1Y + B_2Y^2 + B_3Y^3$

$B_0 = -3.94996e-003$        $B_2 = 8.01435e-003$

$B_1 = 3.66798e+001$        $B_3 = 6.52924e-003$

$Y = \text{Output}$        $X = \text{Load}$

Certificate Number..... 0508290005



(lb)	(mV/V)	
	<u>Compression</u>	
0	0.0000	0.000
15	-0.4065	-0.020
30	-0.8134	-0.026
45	-1.2208	-0.004
60	-1.6277	-0.005
75	-2.0347	0.000
0	0.0009	

ASTM Uncertainty: 0.00067 mV/V

\* Error and Uncertainty were calculated using Straight Line Method in accordance with ASTM E74 with K = 2

Best Fit Equation:  $Y = A_0 + A_1X + A_2X^2 + A_3X^3$   
 $A_0 = -7.00128e-007$      $A_2 = -1.42076e-006$   
 $A_1 = -2.70821e-002$      $A_3 = 1.05788e-008$

Best Fit Equation:  $X = B_0 + B_1Y + B_2Y^2 + B_3Y^3$   
 $B_0 = -2.45077e-005$      $B_2 = -7.11753e-002$   
 $B_1 = -3.69246e+001$      $B_3 = -1.95368e-002$   
 $Y = \text{Output}$      $X = \text{Load}$

Best Fit Equation Was Calculated using the Method of Least Squares.

<u>SHUNT CALIBRATION</u>		
Shunt Value (K ohm)	Output (mV/V)	Load
(lb)		
<u>Tension</u>		
60.4	1.4602	53.6209
<u>Compression</u>		
60.4	1.4602	-53.8231
Shunt Cal is placed across (-E)(-S)		

# Appendix E – Cold Sensor Calibration Certificate

## Certificate of Calibration

**FUTEK**  
Advanced Sensor Technology

Certificate Number..... 0511170009

**Sensor**

Model Number .....	QLA246	Stock No .....	QSH00626
ID Number .....	205689	Capacity .....	250 N

Model: QLA246 - 250 N ()  
Custom Cryogenic Load Cell  
Ver.0 -  
17-4 PH S.S. Standard Cryogenic  
26 Awg 4 Conductor Braided Shielded Teflon Cable - 5 ft.

**Instrument ID:**

Customer Name ..... Jet Propulsion Lab  
Customer Address ..... 4800 Oak Grove Dr, Pasadena CA 91109-8099  
P.O. Number ..... 1277010

**REFERENCE CALIBRATION EQUIPMENT**

**Dead Weight:**

Reference NIST Number: MMAP 822/LA M.S. 12372  
System Cal. Date: 02/20/2004 Next Cal. Date by: 02/20/2009

**Digital Indicator:**

HP Model Number: Agilent 34401A S/N: US36134723  
Cal.Date: January 10, 2005 Next Cal.Date by: January 10, 2006  
Uncertainty Value: 0.0050%

This certifies that the following sensor has been calibrated using equipment traceable to NIST in accordance with FUTEK and applicable to the MIL-STD-45662A. Supporting documentation relative to traceability is on file and is available for examination upon request. This certificate shall not be reproduced except in full, without the written approval of FUTEK

Calibrated By: Angel Mendoza  
Shipment Date: Nov. 17, 2005 Re-Calibration Date: One Year After Shipment Date

LITHO. IN U.S.A.

© 2004 GOES 441

Certificate Number..... 0511170009

**FUTEK**  
Advanced Sensor Technology

**CALIBRATION DATA**

Test Temp ..... 70.00 °F (21.11°C)      Relative Humidity ..... 25.00 %  
Excitation ..... 10 (Vdc)      Input Resistance ..... 746 (Ohms)  
Zero ..... -0.1463 (mV/V)      OutPut Resistance ..... 704 (Ohms)

**Tension**

Rated Output ... 1.6461 mV/V      ZeroReturn .... 0.006% of R.O.  
Linearity ..... 0.057 % of R.O.

**Compression**

Rated Output ... -1.6443 mV/V      ZeroReturn .... -0.009% of R.O.  
Linearity ..... 0.137 % of R.O.

**DATA POINTS**

Load	Output	Non-Lin Error (%)	Hysteresis (%)
(N)	(mV/V)		
		<u>Tension</u>	
0.00	0.0000	0.000	
44.48	0.2927	0.003	
88.96	0.5857	0.025	
133.40	0.8786	0.057	
177.90	1.1713	0.052	
250.20	1.6461	0.000	
0.00	0.0001		

ASTM Uncertainty: 0.00134 mV/V

\* Error and Uncertainty were calculated using Straight Line Method in accordance with ASTM E74 with K = 2

Best Fit Equation:  $Y = A_0 + A_1X + A_2X^2 + A_3X^3$   
A0 = -1.77400e-005      A2 = 1.27365e-007  
A1 = 6.57689e-003      A3 = -4.71214e-010

Best Fit Equation:  $X = B_0 + B_1Y + B_2Y^2 + B_3Y^3$   
B0 = 2.67138e-003      B2 = -4.47887e-001  
B1 = 1.52048e+002      B3 = 2.51708e-001  
Y = Output      X = Load

LITHO. IN U.S.A.

© 2004, CODES 441  
All Rights Reserved

Certificate Number..... 0511170009

**FUTEK**  
Advanced Sensor Technology

(N)	(mV/V)	
	<u>Compression</u>	
0.00	0.0000	0.000
44.49	-0.2933	0.054
88.96	-0.5863	0.100
133.40	-0.8790	0.137
177.90	-1.1711	0.118
250.20	-1.6443	0.000
0.00	0.0001	

ASTM Uncertainty: 0.00351 mV/V

\* Error and Uncertainty were calculated using Straight Line Method in accordance with ASTM E74 with K = 2

Best Fit Equation:  $Y = A_0 + A_1X + A_2X^2 + A_3X^3$

$A_0 = 1.31326e-005$

$A_2 = -2.66821e-008$

$A_1 = -6.59216e-003$

$A_3 = 4.29734e-010$

Best Fit Equation:  $X = B_0 + B_1Y + B_2Y^2 + B_3Y^3$

$B_0 = 1.92198e-003$

$B_2 = -1.00737e-001$

$B_1 = -1.51698e+002$

$B_3 = -2.32981e-001$

Y = Output X = Load

Best Fit Equation Was Calculated using the Method of Least Squares.

**SHUNT CALIBRATION**

Shunt Value (K ohm)	Output (mV/V)	Load
		(N)
		<u>Tension</u>
100	1.7526	266.3850
		<u>Compression</u>
100	1.7526	-266.6817

Shunt Cal is placed across (-E)(-S)

LITHO. IN U.S.A.

© 2004 GOES 441  
All Rights Reserved